

Higgs phenomenology in Type-I 2HDM with $U(1)_H$ Higgs gauge symmetry

P. Ko^a Yuji Omura^b Chaehyun Yu^a

^a*School of Physics, KIAS, 85 Hoegiro, Seoul 130-722, Korea*

^b*Physik Department T30, Technische Universität München,
James-Frank-Straße, 85748 Garching, Germany*

E-mail: pko@kias.re.kr, yuji.omura@tum.de, chyu@kias.re.kr

ABSTRACT: It is well known that generic two-Higgs-doublet models (2HDMs) suffer from potentially large Higgs-mediated flavor-changing neutral current (FCNC) problem, unless additional symmetries are imposed on the Higgs fields thereby respecting the Natural Flavor Conservation Criterion (NFC) by Glashow and Weinberg. A common way to respect the NFC is to impose Z_2 symmetry which is softly broken by a dim-2 operator. Another new way is to introduce local $U(1)_H$ Higgs flavor symmetry that distinguishes one Higgs doublet from the other. In this paper, we consider the Higgs phenomenology in Type-I 2HDMs with the $U(1)_H$ symmetry with the simplest $U(1)_H$ assignments that the SM fermions are all neutral under $U(1)_H$, and we make detailed comparison with the ordinary Type-I 2HDM. After imposing various constraints such as vacuum stability and perturbativity as well as the electroweak precision observables and collider search bounds on charged Higgs boson, we find that the allowed Higgs signal strengths in our model are much broader than those in the ordinary Type-I 2HDM, because of newly introduced $U(1)_H$ -charged singlet scalar and $U(1)_H$ gauge boson. Still the ATLAS data on $gg \rightarrow h \rightarrow \gamma\gamma$ cannot be accommodated. Our model could be distinguished from the ordinary 2HDM with the Z_2 symmetry in a certain parameter region and some channels. If the couplings of the new boson turn out to be close to those in the SM, it would be essential to search for extra $U(1)_H$ gauge boson and/or one more neutral scalar boson to distinguish two models.

Contents

1	Introduction	1
2	Type-I 2HDM with local $U(1)_H$ gauge symmetry	4
2.1	Generalities	4
2.2	Type-I 2HDM with local $U(1)_H$ symmetry	5
2.3	Scalar Potential	6
2.4	Masses and Mixings of Scalar Bosons	7
2.4.1	Charged Higgs (H^\pm)	7
2.4.2	Pseudoscalar boson (A)	7
2.4.3	CP-even scalar bosons (h, H, \tilde{h})	8
2.5	Gauge bosons	8
3	Vacuum Stability Condition and Various Constraints	9
3.1	Vacuum stability condition and perturbative unitarity bounds	9
3.2	Constraints from various experiments	10
3.3	Tree-level ρ parameter	11
3.4	Bound from Z' search in the collider experiments	11
3.5	S , T , and U parameters at the one-loop level	12
3.6	Analysis in 2HDMs with $U(1)_H$ Gauge Symmetry	13
4	Collider phenomenology of the Higgs bosons	16
4.1	Analysis strategies	16
4.2	2HDM with the extra singlet scalar	17
4.3	2HDM with the Z_H boson: fermiophobic case	20
5	Conclusion	22
A	Mass Matrix of CP-even scalars	24

1 Introduction

The new boson discovered at the Large Hadron Collider (LHC) in the mass range 125–126 GeV [1, 2] provides the missing link responsible for the origin of electroweak symmetry breaking and the masses of the Standard Model (SM) particles. Recent analyses for the spin and parity of this new boson at ATLAS and CMS exclude the hypothesis that this boson has different spin or parity from the SM Higgs boson by over 93% C.L. or higher [3, 4]. Although there are controversial observations for the decay of the scalar boson, such as the excess of the branching ratio for $h \rightarrow \gamma\gamma$ at ATLAS, the most updated values of couplings of this boson to the SM particles observed at the LHC indicate that this new boson is very

close to the SM Higgs boson. Then the next natural question on the scalar boson would be whether it is exactly the same as the SM Higgs boson, or one of Higgs bosons in Beyond SM with extended scalar sector.

One of the simplest extensions of the SM Higgs sector is the two-Higgs-doublet model (2HDM), where an extra Higgs $SU(2)_L$ doublet is added to the SM Higgs sector. This extension may be motivated by many new physics models like the supersymmetric Standard Model, grand unified theories (GUTs), and so on. Many interesting physics issues have been studied in detail within 2HDMs (see Ref. [5] for recent reviews).

However, the new scalars generally allow tree-level flavor-changing neutral currents (FCNCs) through the Yukawa couplings with SM fermions, and would be in conflict with observations that FCNC processes are highly suppressed in Nature, unless the scalars with flavor-changing tree-level couplings are heavy enough.*

One way to avoid this Higgs-mediated flavor problem is the so-called Natural Flavor Conservation (NFC), where fermions of the same electric charges get their masses from one Higgs vacuum expectation value (VEV) [6]. One can assign new distinct charges to the two Higgs doublets as well as to the SM fermions so that the NFC criterion can be achieved. Then the resulting Yukawa couplings involving the neutral scalars would not allow the tree-level FCNCs mediated by neutral Higgs bosons.

In most cases, a softly broken discrete Z_2 symmetry is imposed in the 2HDMs [6]. Two Higgs doublets, H_1 and H_2 , have different Z_2 parity, and only couplings following minimal flavor violation (MFV) are allowed. The 2HDMs with softly broken Z_2 symmetry *à la* the proposal of Glashow and Weinberg have been widely discussed in the literature, and a lot of interesting signals can be predicted without serious conflicts with experiments involving FCNCs. However, the predicted extra scalars in the 2HDMs are strongly constrained by the collider search and the explicit Z_2 symmetry breaking terms tend to be required to shift the pseudoscalar mass. Although this approach has been widely adopted in multi-Higgs doublet models, it is not clear what are the origins of the discrete Z_2 symmetry and its soft breaking.

Recently the present authors proposed a new resolution of the Higgs-mediated FCNC problem in 2HDMs, by implementing the usual softly broken discrete Z_2 symmetry to spontaneously broken local $U(1)_H$ symmetry [7]†. Two Higgs doublets H_1 and H_2 have different $U(1)_H$ charges, and each SM fermion carries its own $U(1)_H$ charge in such a way that the phenomenologically viable Yukawa couplings are allowed without too excessive Higgs-mediated FCNC in a similar way to the usual 2HDMs with softly broken Z_2 symmetry. The gauged $U(1)_H$ symmetry could realize such a large pseudo-scalar mass by spontaneous breaking of $U(1)_H$ gauge symmetry introducing a new SM singlet scalar Φ with nonzero $U(1)_H$ charge. Then the local $U(1)_H$ symmetry is spontaneously broken into the softly broken Z_2 symmetry. In other words, the 2HDMs with spontaneously broken local $U(1)_H$ symmetry could be the origin of the usual 2HDMs with softly broken Z_2 sym-

*The FCNC problem mediated by the neutral Higgs boson may be resolved in some specific models, where, for instance, the neutral Higgs couplings are naturally suppressed by the Cabibbo-Kobayashi-Maskawa matrix (V_{CKM}) [8] or the Yukawa couplings are aligned in flavor space [9].

† See Ref. [10] for supersymmetric extension of the SM with extra gauge interactions including $U(1)_H$.

metry with the NFC criterion by Glashow and Weinberg. In Ref. [7], the authors discussed in detail how to build new 2HDMs with local $U(1)_H$ Higgs symmetry. In the type-I model, it is possible to construct an anomaly-free model without extra chiral fermions by assigning appropriate $U(1)_H$ charges to the SM fermions and right-handed neutrino as in Table I. It was also shown that the type-II 2HDM with local $U(1)_H$ symmetry could be interpreted as the effective theory of the E_6 GUT model with leptophobic Z' boson [11, 12]. These are new and amusing results, and the concept of local $U(1)_H$ Higgs gauge symmetry widely opens new possibilities for the multi-Higgs-doublet models.

The SM fermions are very often chiral under the $U(1)_H$ gauge symmetry proposed in Ref. [7], and the issues of anomaly cancellation and realistic Yukawa couplings have to be addressed carefully before one starts phenomenology. In general, there appears gauge anomaly once extra gauge symmetry is added, so that extra chiral fermions are also required. Also one may have to introduce new Higgs doublets which are charged under new gauge groups, in order to write realistic Yukawa couplings. When one discusses phenomenology in the extended SM with extra gauge symmetry, one must consider all ingredients to make theory consistent, even though some of them might be irrelevant at the electroweak energy scale. This procedure to include all ingredients to consist of phenomenological theory was emphasized in the chiral $U(1)'$ models with flavored Higgs doublets, which could accommodate the large deviation in the top quark forward-backward asymmetry at the Tevatron with the SM prediction [13–16].

Another new interpretation of the local $U(1)_H$ Higgs gauge symmetry proposed in Ref. [7] is also possible. Suppose there is a new chiral local gauge symmetry in nature (to say, $U(1)_\chi$ for simplicity), under which some of the SM fermions are also charged. Then it may be mandatory to extend the Higgs sector by introducing a new Higgs doublet which is charged under the new chiral $U(1)_\chi$ gauge symmetry. This is because in general one cannot write down the Yukawa couplings for all the SM fermions without $U(1)_\chi$ -charged Higgs doublets. The $U(1)_\chi$ charge of the Higgs doublet should match those of the SM chiral fermions in order to respect local $U(1)_\chi$ gauge symmetry. There would be infinitely many possible choices for the $U(1)_\chi$ assignments which are also anomaly-free. However not all of them would be phenomenologically viable because of the Higgs-mediated FCNC problem. Only a subset of anomaly-free chiral $U(1)_\chi$ models with multi-Higgs-doublet models would satisfy the NFC criterion. Our construction in Ref. [7] can be regarded as finding new chiral $U(1)_\chi$ models which meet anomaly cancellation and the NFC *à la* Glashow and Weinberg.

In this paper, we extend our previous work about the new 2HDMs with $U(1)_H$ Higgs symmetry [7]. In the previous work, we proposed $U(1)_H$ charge assignments and full matter contents corresponding to each type of 2HDMs. Since a SM-like Higgs boson was discovered at the LHC, it would be timely to discuss if our 2HDMs with local $U(1)_H$ symmetry would be consistent with the Higgs observation at the LHC. After the discovery of the SM-like Higgs boson at the LHC, a lot of works have been carried out in the context of the ordinary 2HDM of Type-I, Type-II, Type-X, and Type-Y [17–34]. In this work, we will mainly concentrate on the simplest case, the type-I 2HDM with $U(1)_H$ gauge symmetry, and compare our model with the ordinary type-I 2HDM. In the type-I 2HDM case, only one Higgs doublet couples to the SM fermions and the other Higgs doublet and

singlet do not couple to them. In the type-I 2HDM with $U(1)_H$ symmetry, we can achieve anomaly-free models without extra chiral fermions. Furthermore, constraints from flavor physics and the collider experiments could be relaxed drastically (see Secs. 3 and 4).

This paper is organized as follows. In Sec. 2, we recapitulate the Type-I 2HDM with the spontaneous $U(1)_H$ Higgs gauge symmetry breaking including the general Higgs potential, and discuss the vacuum stability condition for the Higgs potential. Then we derive the physical states of the Higgs fields and the masses of the $SU(2)$ gauge bosons in terms of the gauge coupling and Higgs VEVs and discuss the bounds on the physical masses of the charged Higgs and neutral Higgs bosons. Section 3 is devoted to the discussion of the constraints derived from electroweak precision observables (EWPOs), and the comparison of our model with the usual Type-I 2HDM. (The results obtained in Sec. 3 involves only gauge couplings of two Higgs doublets and could be applied to and shared with other types of 2HDM [35].) Then we discuss phenomenology of Higgs bosons in our model at the LHC in Sec. 4. Conclusion of this paper is given in Sec. 5. We present some useful formulas in Appendix.

2 Type-I 2HDM with local $U(1)_H$ gauge symmetry

2.1 Generalities

In 2HDMs, symmetry to distinguish the two $SU(2)_L$ Higgs doublets is required in order to avoid tree-level FCNCs. One usually assign Z_2 parities to two Higgs doublets and the SM fermion fields [6] to achieve the NFC by Glashow and Weinberg. Depending on the charge assignment, one can obtain so-called Type-I 2HDM, Type-II 2HDM, and etc.. Since the Yukawa couplings of the SM fermions are controlled by the Z_2 parities, the models allow the couplings respecting the hypothesis of MFV.

In the usual 2HDMs with the softly broken Z_2 symmetry, there are extra physical scalar bosons: one extra CP-even scalar (H), one pseudoscalar (A), and one charged Higgs pair (H^\pm). The scalar masses are given by the Higgs VEVs and dimensionless couplings in the Higgs potential at the renormalizable level. Therefore we can expect that the mass scales of all extra scalar bosons are around the electroweak (EW) scale, like the SM-like Higgs boson observed at the LHC. However, the masses and couplings of the extra scalar bosons are strongly constrained by the collider experiments and the EWPOs as well as the constraints from the flavor physics. One has to introduce the Z_2 symmetry breaking term (soft breaking via dim-2 operators), which generates the pseudo scalar mass (m_A), in order to consider the higher mass scales.

In Ref. [7], the present authors proposed gauged $U(1)_H$ symmetry, which may be considered as the origin of the Z_2 symmetry, and constructed a number of well-defined extensions of 2HDMs with only MFV. In this case, the pseudo scalar mass m_A is generated by spontaneous symmetry breaking of $U(1)_H$ via nonzero VEV of a new $U(1)_H$ -charged singlet scalar Φ . The Lagrangian for the two Higgs (H_i ($i = 1, 2$)) and an extra $U(1)_H$ -

charged scalar (Φ) is

$$\mathcal{L}_H = \sum_{i=1}^2 \left| \left(D_\mu^{SM} - ig_H q_{H_i} \hat{Z}_{H\mu} \right) H_i \right|^2 + \left| \left(\partial_\mu - ig_H q_\Phi \hat{Z}_{H\mu} \right) \Phi \right|^2 - V_{\text{scalar}}(H_1, H_2, \Phi) + \mathcal{L}_{\text{Yukawa}}, \quad (2.1)$$

where D_μ^{SM} is the covariant derivatives for H_i under the SM-gauge groups. g_H is the $U(1)_H$ gauge coupling, and q_{H_i} and q_Φ are $U(1)_H$ charges of H_i 's and Φ , respectively. V_{scalar} is the scalar potential for H_i and Φ which breaks $U(1)_H$ and the EW symmetry. And $\hat{Z}_{H\mu}$ is the $U(1)_H$ gauge boson in the interaction eigenstates. Finally $\mathcal{L}_{\text{Yukawa}}$ is the Yukawa interaction between the SM fermions and the two Higgs doublets, which would be the same as the Yukawa interactions in Type-I, Type-II, etc..[‡]

This extension might suffer from tree-level deviation of the ρ parameter due to the kinetic and mass mixings between the $U(1)_H$ gauge boson and Z boson. Furthermore, this extension would modify relevant collider signatures because of the additional Higgs doublet as well as the extra gauge boson Z_H and the complex scalar Φ .

2.2 Type-I 2HDM with local $U(1)_H$ symmetry

There are many different ways to assign $U(1)_H$ charges to the SM fermions to achieve the NFC in 2HDMs with local $U(1)_H$ gauge symmetry. The phenomenology will crucially depend on the $U(1)_H$ charge assignments of the SM fermions. In general, the models will be anomalous, even if $U(1)_H$ charge assignments are non-chiral, so that one has to achieve anomaly cancellation by adding new chiral fermions to the particle spectrum.

Type	U_R	D_R	Q_L	L	E_R	N_R	H_2
$U(1)_H$ charge	u	d	$\frac{(u+d)}{2}$	$\frac{-3(u+d)}{2}$	$-(2u+d)$	$-(u+2d)$	$q_{H_2} = \frac{(u-d)}{2}$
$q_{H_1} \neq 0$	0	0	0	0	0	0	0
$U(1)_{B-L}$	1/3	1/3	1/3	-1	-1	-1	0
$U(1)_R$	1	-1	0	0	-1	1	1
$U(1)_Y$	2/3	-1/3	1/6	-1/2	-1	0	1/2

Table 1. Charge assignments of an anomaly-free $U(1)_H$ in the Type-I 2HDM.

For the Type-I case, the present authors noticed that one can achieve an anomaly-free $U(1)_H$ assignment even without additional chiral fermions as in Table 1. Only H_2 couples with the SM fermions, and the $U(1)_H$ charges of $H_{1,2}$, q_{H_1} and q_{H_2} , should be different. Since the $U(1)_H$ charges of right-handed up- and down-type quarks (u and d) in Table 1 are arbitrary, one can construct an infinite number of new models from the usual Type-I 2HDM by implementing the softly broken Z_2 symmetry to spontaneously broken local $U(1)_H$ gauge symmetry. In the heavy Z_H limit, all the models with Type-I models with local $U(1)_H$ with arbitrary u and d will get reduced to the conventional Type-I 2HDM with softly broken Z_2 term (see m_3^2 term in Eq. (2) in the next subsection). In

[‡]We ignore the kinetic mixing between $U(1)_H$ and $U(1)_Y$ for simplicity in this paper.

Table 1, we present four interesting $U(1)_H$ charge assignments: the fermiophobic $U(1)_H$ with $u = d = 0$, $U(1)_{B-L}$, $U(1)_R$, and $U(1)_Y$ cases.

2.3 Scalar Potential

The scalar potential of general 2HDMs with $U(1)_H$ is completely fixed by local gauge invariance and renormalizability, and given by

$$\begin{aligned} V_{\text{scalar}} = & \hat{m}_1^2(|\Phi|^2)H_1^\dagger H_1 + \hat{m}_2^2(|\Phi|^2)H_2^\dagger H_2 - \left(m_3^2(\Phi)H_1^\dagger H_2 + h.c.\right) \\ & + \frac{\lambda_1}{2}(H_1^\dagger H_1)^2 + \frac{\lambda_2}{2}(H_2^\dagger H_2)^2 + \lambda_3(H_1^\dagger H_1)(H_2^\dagger H_2) + \lambda_4|H_1^\dagger H_2|^2 \\ & + m_\Phi^2|\Phi|^2 + \lambda_\Phi|\Phi|^4. \end{aligned} \quad (2.2)$$

Φ is a complex singlet scalar with $U(1)_H$ charge, q_Φ , and contributes to the $U(1)_H$ symmetry breaking. $\hat{m}_i^2(|\Phi|^2)$ ($i = 1, 2$) and $m_3^2(\Phi)$ could be functions of Φ : $\hat{m}_i^2(|\Phi|^2) = m_i^2 + \tilde{\lambda}_i|\Phi|^2$ at the renormalizable level. $m_3^2(\Phi)$ is fixed by q_{H_1} and q_Φ , and $m_3^2(\langle\Phi\rangle) = 0$ is satisfied at $\langle\Phi\rangle = 0$: $m_3^2(\Phi) = \mu\Phi^n$, where n is defined as $n = (q_{H_1} - q_{H_2})/q_\Phi$. A mass parameter μ can be regarded as real by suitable redefinition of the phase of Φ . Note that the λ_5 term ($\frac{1}{2}\lambda_5[(H_1^\dagger H_2)^2 + h.c.]$) in the usual 2HDMs with softly broken Z_2 symmetry does not appear in our models, because we impose the local $U(1)_H$ gauge symmetry instead of Z_2 . In our model, the effective λ_5 term would be generated from the scalar exchange, after $U(1)_H$ symmetry breaking. The effective λ_5 would contribute to the pseudoscalar mass, the vacuum stability and unitarity conditions like the ordinary 2HDMs. [§]

Expanding the scalar fields around their vacua,

$$\langle H_i^T \rangle = (0, v_i/\sqrt{2}), \quad \langle \Phi \rangle = v_\Phi/\sqrt{2},$$

one can study the physical spectra in the scalar sector including their masses and couplings. The neutral scalars, h_i, χ_i, h_Φ , and χ_Φ , and the charged Higgs, ϕ_i^\pm , in the interaction eigenstates are defined by

$$H_i = \begin{pmatrix} \phi_i^+ \\ \frac{v_i}{\sqrt{2}} + \frac{1}{\sqrt{2}}(h_i + i\chi_i) \end{pmatrix}, \quad \Phi = \frac{1}{\sqrt{2}}(v_\Phi + h_\Phi + i\chi_\Phi). \quad (2.3)$$

The scalar VEVs v_i and v_Φ satisfy the stationary conditions (or vanishing tadpole conditions):

$$0 = m_1^2 v_1 - m_3^2 v_2 + \lambda_1 \frac{v_1^3}{2} + \lambda_3 \frac{v_1 v_2^2}{2} + \lambda_4 \frac{v_1 v_2^2}{2}, \quad (2.4)$$

$$0 = m_2^2 v_2 - m_3^2 v_1 + \lambda_2 \frac{v_2^3}{2} + \lambda_3 \frac{v_2 v_1^2}{2} + \lambda_4 \frac{v_2 v_1^2}{2}, \quad (2.5)$$

$$0 = \frac{v_\Phi}{2}(\tilde{\lambda}_1 v_1^2 + \tilde{\lambda}_2 v_2^2) - m_3'^2(v_\Phi) \frac{v_1 v_2}{\sqrt{2}} + m_\Phi^2 v_\Phi + \lambda_\Phi v_\Phi^3, \quad (2.6)$$

with $m_3'^2(v_\Phi) \equiv \partial_\Phi m_3^2(v_\Phi)$.

[§]The coupling λ_5 could also be generated by the dimension six operator $\lambda_5'[(H_1^\dagger H_2)^2 \Phi^2 + h.c.]$. Then we have to keep all the possible dimension-6 operators in the scalar potential in order to analyze the physical spectra which is a formidable task, and we would lose the predictability. In this paper, we consider only the renormalizable lagrangian and just ignore higher dimensional operators for simplicity and predictability.

2.4 Masses and Mixings of Scalar Bosons

In 2HDMs with $U(1)_H$ and Φ , there are three CP-even scalars, one pseudoscalar, and one charged Higgs pair after $U(1)_H$ and EW symmetry breaking. There is also an additional massless scalar corresponding to $U(1)_H$ breaking, which is eaten by the additional gauge boson of $U(1)_H$, called Z_H . Without $U(1)_H$ -charged Φ , the two CP-odd scalars in H_i could be eaten by the gauge bosons, so that we could discuss the effective model with no massive pseudoscalar and $U(1)_H$ gauge boson [7, 36]. One may consider a model with Z_2 Higgs symmetry instead of $U(1)_H$. In this case, Φ should be a scalar to avoid a massless mode and three CP-even scalars will appear after the symmetry breaking. Both cases will correspond to some limits of the 2HDM with $U(1)_H$ and Φ .

2.4.1 Charged Higgs (H^\pm)

After the EW symmetry breaking, one Goldstone pair (G^\pm) and one massive charged Higgs pair (H^\pm) appear. The directions of Goldstone bosons are fixed by the Higgs VEVs:

$$\begin{pmatrix} \phi_1^+ \\ \phi_2^+ \end{pmatrix} = \begin{pmatrix} \cos \beta \\ \sin \beta \end{pmatrix} G^+ + \begin{pmatrix} -\sin \beta \\ \cos \beta \end{pmatrix} H^+, \quad (2.7)$$

where $(v_1, v_2) = (v \cos \beta, v \sin \beta)$ and $v = \sqrt{v_1^2 + v_2^2}$. The squared mass of the charged Higgs boson H^+ is given by

$$m_{H^+}^2 = \frac{m_3^2}{\cos \beta \sin \beta} - \lambda_4 \frac{v^2}{2}. \quad (2.8)$$

In the 2HDM without Φ , m_3^2 is zero and $m_{H^+}^2$ is determined only by the second term with negative λ_4 . In the 2HDM with Φ , λ_4 could be either negative or positive.

2.4.2 Pseudoscalar boson (A)

In 2HDMs with discrete Z_2 symmetry, one CP-odd mode is eaten by the Z boson and the other becomes massive. In the 2HDM with a complex scalar, Φ , there is an additional CP-odd mode and two Goldstone bosons ($G_{1,2}$) appear after the EW and $U(1)_H$ symmetry breaking. $m_3^2(\Phi)$ plays a crucial role in the mass of A , m_A . $m_3^2(\Phi)$ is $m_3^2(\Phi) = \mu\Phi$ or $\mu\Phi^2$ in the renormalizable potential depending on the definition of $q_\Phi = (q_{H_1} - q_{H_2})$ or $(q_{H_1} - q_{H_2})/2$.

The directions of $G_{1,2}$ and A are defined as

$$\begin{aligned} \begin{pmatrix} \chi_\Phi \\ \chi_1 \\ \chi_2 \end{pmatrix} &= \begin{pmatrix} 0 \\ \cos \beta \\ \sin \beta \end{pmatrix} G_1 + \frac{v_\Phi}{\sqrt{v_\Phi^2 + (nv \cos \beta \sin \beta)^2}} \begin{pmatrix} 1 \\ \frac{nv}{v_\Phi} \cos \beta \sin^2 \beta \\ -\frac{nv}{v_\Phi} \cos^2 \beta \sin \beta \end{pmatrix} G_2 \\ &+ \frac{v_\Phi}{\sqrt{v_\Phi^2 + (nv \cos \beta \sin \beta)^2}} \begin{pmatrix} \frac{nv}{v_\Phi} \cos \beta \sin \beta \\ -\sin \beta \\ \cos \beta \end{pmatrix} A. \end{aligned} \quad (2.9)$$

The squared pseudoscalar mass m_A^2 is given by

$$m_A^2 = \frac{m_3^2}{\cos \beta \sin \beta} \left(1 + \frac{n^2 v^2}{v_\Phi^2} \cos^2 \beta \sin^2 \beta \right), \quad (2.10)$$

where $n = 1$ or 2 depending on $m_3^2(\Phi)$. G_1 corresponds to the Goldstone boson in the ordinary 2HDMs and could be eaten by the Z boson. In the limit, $v_\Phi \rightarrow \infty$, χ_Φ is G_2 and eaten by Z_H . Also the direction of A and m_A^2 become the same as in the ordinary 2HDMs. In the 2HDM with local $U(1)_H$ symmetry but without Φ , A does not exist, so that it could corresponds to the limit, $m_A \rightarrow \infty$ and $v_\Phi \rightarrow 0$. In the following section, we discuss our 2HDMs assuming $m_3^2(\Phi) = \mu\Phi$ and $q_\Phi = (q_{H_1} - q_{H_2})$.

2.4.3 CP-even scalar bosons (h, H, \tilde{h})

After the EW and $U(1)_H$ symmetry breaking, three massive CP-even scalars appear and they generally mix with each other as follows:

$$\begin{pmatrix} h_\Phi \\ h_1 \\ h_2 \end{pmatrix} = \begin{pmatrix} 1 & 0 & 0 \\ 0 & \cos \alpha & -\sin \alpha \\ 0 & \sin \alpha & \cos \alpha \end{pmatrix} \begin{pmatrix} \cos \alpha_1 & 0 & -\sin \alpha_1 \\ 0 & 1 & 0 \\ \sin \alpha_1 & 0 & \cos \alpha_1 \end{pmatrix} \begin{pmatrix} \cos \alpha_2 & -\sin \alpha_2 & 0 \\ \sin \alpha_2 & \cos \alpha_2 & 0 \\ 0 & 0 & 1 \end{pmatrix} \begin{pmatrix} \tilde{h} \\ H \\ h \end{pmatrix}, \quad (2.11)$$

where α corresponds to the mixing angle between two neutral scalars in the ordinary 2HDM and $\alpha_{1,2}$ are additional mixing angles that newly appear in our model with local $U(1)_H$ and a singlet scalar Φ . The mixing is given by the mass matrix which is introduced in Appendix A. In the limit of $\alpha_{1,2} \rightarrow 0$ one can interpret h_Φ as the field in the mass basis and h_Φ does not mix with $h_{1,2}$. Throughout this paper, we assume that h is the SM-like scalar boson with its mass (m_h) being fixed around 126 GeV.

2.5 Gauge bosons

In 2HDMs with local $U(1)_H$ Higgs symmetry, at least one of the Higgs doublets $H_{i=1,2}$ should be charged under $U(1)_H$. Therefore tree-level mass mixing between Z and Z_H would appear after spontaneous breaking of the EW and $U(1)_H$ symmetries. Let us describe the mass matrix of Z and Z_H as

$$\begin{pmatrix} \hat{M}_Z^2 & \Delta M_{ZZ_H}^2 \\ \Delta M_{ZZ_H}^2 & \hat{M}_{Z_H}^2 \end{pmatrix}. \quad (2.12)$$

\hat{M}_Z^2 and $\hat{M}_{Z_H}^2$ are

$$\hat{M}_Z^2 = \frac{g^2 + g'^2}{4} v^2 = \frac{g_Z^2}{4} v^2, \quad \hat{M}_{Z_H}^2 = g_H^2 \left\{ \sum_{i=1}^2 (q_{H_i} v_i)^2 + q_\Phi^2 v_\Phi^2 \right\}, \quad (2.13)$$

and the mass mixing term between Z and Z_H is

$$\Delta M_{ZZ_H}^2 = -\frac{\hat{M}_Z}{v} g_H \sum_{i=1}^2 q_{H_i} v_i^2. \quad (2.14)$$

Here g, g' and g_H are the gauge couplings of $U(1)_Y$, $SU(2)_L$, and $U(1)_H$ gauge interactions, respectively. And q_{H_i} and q_Φ are the $U(1)_H$ charges of the Higgs doublet H_i 's and the singlet scalar Φ , respectively. Some examples of the charge assignments within Type-I 2HDM are shown in Table 1. $U(1)_H$ charge assignments for other types of 2HDMs can be found in Ref. [7].

The tree-level masses in the mass eigenstates are given by

$$M_{Z0}^2 = \frac{1}{2} \left\{ \hat{M}_{Z_H}^2 + \hat{M}_Z^2 - \sqrt{(\hat{M}_{Z_H}^2 - \hat{M}_Z^2)^2 + 4\Delta M_{ZZ_H}^4} \right\}, \quad (2.15)$$

$$M_{Z_H0}^2 = \frac{1}{2} \left\{ \hat{M}_Z^2 + \hat{M}_{Z_H}^2 + \sqrt{(\hat{M}_{Z_H}^2 - \hat{M}_Z^2)^2 + 4\Delta M_{ZZ_H}^4} \right\}. \quad (2.16)$$

Then the mixing between Z and Z_H is described by the mixing angle ξ , which is defined as

$$\tan 2\xi = \frac{2\Delta M_{ZZ_H}^2}{\hat{M}_{Z_H}^2 - \hat{M}_Z^2}. \quad (2.17)$$

Note that we omit the symbol “0” for the physical (renormalized) masses for the gauge bosons. The extra gauge boson couples with the SM fermions through the mixing even if the SM fermions are not charged under $U(1)_H$. Furthermore, this mixing modifies the coupling of the Z boson with the fermions, which has been well-investigated at the LEP experiments. The Z boson mass is also deviated from the SM prediction according to Eq. (2.15) and the allowed size of the deviation is evaluated by the ρ parameter. Our 2HDMs are strongly constrained not only by the Z_H search in the experiments but also by the EWPOs, as we will see in the next section.

3 Vacuum Stability Condition and Various Constraints

3.1 Vacuum stability condition and perturbative unitarity bounds

There are many theoretical and experimental constraints on our model. First we consider theoretical bounds on Higgs self couplings from vacuum stability condition and perturbative unitarity.

In order to break the $U(1)_H$ and EW symmetry, the potential (2.2) should have a stable vacuum with nonzero VEVs, namely the scalar potential is bounded from below. We impose the vacuum stability bounds, which require that the dimensionless couplings $\lambda_{1,2,3,4}$ are to satisfy the following conditions:

$$\lambda_1 > 0, \lambda_2 > 0, \lambda_3 > -\sqrt{\lambda_1\lambda_2}, \lambda_3 + \lambda_4 > -\sqrt{\lambda_1\lambda_2}, \quad (3.1)$$

in the $\langle \Phi \rangle = 0$ direction. They correspond to the ones in the usual 2HDMs without λ_5 . Following the conditions and Eq. (A.11) in Appendix A, the masses of scalars satisfy

$$m_h^2 + m_H^2 - m_A^2 > 0. \quad (3.2)$$

In the ordinary 2HDMs with softly broken Z_2 symmetry, sizable λ_5 is allowed and the conditions (3.1) and (3.2) should be modified by the replacements, $m_{H+}^2 \rightarrow m_{H+}^2 + \lambda_5 v^2$, $m_A^2 \rightarrow m_A^2 + \lambda_5 v^2$ and $\lambda_4 \rightarrow \lambda_4 - |\lambda_5|$ in Eqs. (2.8), (3.1), and (3.2).

In the $\langle \Phi \rangle \neq 0$ direction, the vacuum-stability conditions for λ_Φ , $\widetilde{\lambda}_1$ and $\widetilde{\lambda}_2$ are

$$\begin{aligned} \lambda_\Phi > 0, \quad \lambda_1 > \frac{\widetilde{\lambda}_1^2}{\lambda_\Phi}, \quad \lambda_2 > \frac{\widetilde{\lambda}_2^2}{\lambda_\Phi}, \quad \lambda_3 - \frac{\widetilde{\lambda}_1 \widetilde{\lambda}_2}{\lambda_\Phi} > -\sqrt{\left(\lambda_1 - \frac{\widetilde{\lambda}_1^2}{\lambda_\Phi}\right) \left(\lambda_2 - \frac{\widetilde{\lambda}_2^2}{\lambda_\Phi}\right)}, \\ \lambda_3 + \lambda_4 - \frac{\widetilde{\lambda}_1 \widetilde{\lambda}_2}{\lambda_\Phi} > -\sqrt{\left(\lambda_1 - \frac{\widetilde{\lambda}_1^2}{\lambda_\Phi}\right) \left(\lambda_2 - \frac{\widetilde{\lambda}_2^2}{\lambda_\Phi}\right)}, \end{aligned} \quad (3.3)$$

where the directions of H_1 and H_2 fields in the last four conditions are the same as those of H_1 and H_2 fields in Eq. (3.1).

We also impose the perturbativity bounds $\lambda_i \leq 4\pi$ on the quartic Higgs couplings and the tree-level unitarity conditions whose expressions are given in Ref. [37–39]. These will make theoretical constraints on the quartic couplings in the scalar potential (2).

3.2 Constraints from various experiments

The charged Higgs boson mass is constrained by the LEP experiments. It depends on the decay channel of the charged Higgs boson, and we take the model-independent bound $m_{h^\pm} \gtrsim 80$ GeV [40] in this work. We also impose a recent bound on the charged Higgs and $\tan \beta$ coming from the top quark decay from the LHC experiments [41–43]. We note that the flavor bound which mainly comes from the $b \rightarrow s\gamma$ experiments is $\tan \beta \gtrsim 1$ in the type-I 2HDM [44].

Recently the BABAR Collaboration reported about 3.4σ deviation from the SM prediction in the $B \rightarrow D^{(*)}\tau\nu$ decays [45]. This deviation cannot be accommodated with the ordinary 2HDM with MFV in the Yukawa sector. It turned out that 2HDMs which violate MFV might account for the discrepancy. The chiral $U(1)'$ model with flavored Higgs doublets which slightly breaks the NFC criteria in the right-handed up-type quark sector [16] is one of such examples. Since the 2HDMs with $U(1)_H$ hold the MFV hypothesis, they cannot be accommodated with the deviation in $B \rightarrow D^{(*)}\tau\nu$. In this work, we do not consider these experiments seriously since the experimental results are not well settled down. In the future, if this deviation would be confirmed at Belle or Belle II, it might exclude our 2HDMs as well as the ordinary 2HDMs.

EWPOs in the LEP experiments which are usually parametrized by Peskin-Takeuchi parameters S , T , and U [46] provides strong bounds on the parameters in the Higgs potential. If new physics has no direct couplings to the SM fermions, their effects at the LEP energy scale would appear only through the self energies of $SU(2)_L$ gauge bosons. This is the case of the usual Type-I 2HDM. However, in our model there exists a new $U(1)_H$ gauge boson, which may couple to the SM fermions. In this case, one must consider all observables at the Z pole at the one-loop level instead of S , T , and U [47]. However if the new gauge boson is decoupled from the EW scale physics, S , T , and U will provide well-defined constraints on the 2HDMs with $U(1)_H$. We will discuss this bound in a few next subsections.

3.3 Tree-level ρ parameter

If the Higgs doublets are charged under the extra gauge symmetry, the extra symmetry would also be broken along with EW symmetry breaking. Then there appears the mass mixing between the Z boson and the extra massive gauge boson. In the 2HDMs with $U(1)_H$, the mixing between Z and Z_H is generated as in Eq. (2.17). This mass mixing could allow the Z boson mass to deviate significantly from the SM prediction, and thus will strongly be constrained by the ρ parameter, which the SM predicts to be one at the tree level.

Assuming $\xi \ll 1$, the tree-level ρ parameter is described as

$$\rho = 1 + \frac{\Delta M_{ZZ_H}^2}{M_{Z_0}^2} \xi + O(\xi^2). \quad (3.4)$$

The mixing also changes the Z boson couplings with the SM fermions and the factor is estimated as $1 - \xi^2/2$.

The bounds on the tree-level mixing have been discussed in Refs. [48–50]. As we will see in Fig. 1 (a), we can derive the bounds on g_H , $\tan\beta$, and M_{Z_H} in the case with $(q_{H_1}, q_{H_2}) = (1, 0)$, when we require that the tree-level contributions to the ρ parameter and the decay width of the Z boson, which are functions of the Z -boson couplings, are within the error of the SM predictions: $\rho = 1.01051 \pm 0.00011$ and $\Gamma_Z = 2.4961 \pm 0.0010$ GeV [51]. The tree-level deviations may also affect the S , T , and U parameters, but they actually become negligible because of the requirement for the stringent bound from Z' search at the LHC, as we discuss in the next section.

3.4 Bound from Z' search in the collider experiments

Extra neutral gauge bosons are strongly constrained by Z' searches at high energy colliders. In our models, Z_H can couple with the SM fermions through the Z - Z_H mixing, even if we choose the charged assignment that the SM fermions are not charged under $U(1)_H$.

If Z_H couples with leptons, especially electron and muon, Z_H would be produced easily at LEP and the coupling and mass of Z_H are strongly constrained by the experimental results, which are consistent with the SM prediction with very high accuracy. If Z_H is heavier than the center-of-mass energy of LEP (209 GeV), we could derive the bound on the effective coupling of Z_H [52–54]. The lower bound on M_{Z_H}/g_H would be $O(10)$ TeV [53, 54]. If Z_H is lighter than 209 GeV, the upper bound of Z_H coupling would be $O(10^{-2})$ to avoid conflicts with the data of $e^+e^- \rightarrow f^-f^+$ ($f = e, \mu$) [51, 53, 54].

Furthermore, there will be strong bounds from hadron colliders, if quarks are charged under $U(1)_H$. The upper bounds on the Z_H production at the Tevatron and LHC are investigated in the processes, $pp(\bar{p}) \rightarrow Z_H X \rightarrow f\bar{f}X$ [51, 52, 55, 56], and the stringent bound requires $O(10^{-3})$ times smaller couplings than the Z -boson couplings for $M_{Z'} \leq 1$ TeV [56].

We could avoid these strong constraints, in the case that all particles except for one Higgs doublet are not charged under $U(1)_H$. Actually the model in the first row of Table 1 is this case. Z_H couples with the SM fermions only through the Z - Z_H mixing, so that the

mixing should be sufficiently small. In the following sections, we focus on the fermiophobic $U(1)_H$ charge assignment and require the (conservative) bound $\sin \xi \lesssim 10^{-3}$, according to Ref. [56]. The small mixing especially contributes to the T parameter as $\alpha T \sim \rho - 1$, but it will not affect our results.

In the 2HDM with $U(1)_H$, Z_H can decay to Z and scalars, so that the strong bound, $\sin \xi \lesssim 10^{-3}$, will be relaxed if the branching ratio of the Z_H decay into Z and scalars is almost one. In the following sections, we study the region with $M_{Z_H} \leq 1\text{TeV}$, and the additional branching ratio is at most 0.1 in that region. If we assume that there are extra particles charged under $U(1)_H$ and Z_H mainly decays to the extra particles, the larger value for $\sin \xi$ could be allowed. We note that the constraint from the Z' search in the dijet production at the LHC can easily be avoided by the bound on the mixing angle ξ .

In the region of $M_{Z_H} > 1\text{TeV}$, the constraints from the Z' search are relaxed and the constraint on $g_H \cos \beta$ from the ρ parameter and Γ_Z becomes stronger as we will see in Fig. 1 (a).

3.5 S , T , and U parameters at the one-loop level

Here, we introduce S , T , and U parameters in the 2HDMs with the $U(1)_H$ gauge boson and Φ at the one-loop level. They involve only gauge interactions of scalars, so that the results could be applied to other types of 2HDMs [35]. The EWPOs in 2HDMs with extra scalars have been calculated in Refs.[57, 58].

In order to calculate the S , T , and U parameters, we define mass eigenstates $\{H_l^+\}$, $\{H_l\}$, and $\{A_l\}$ of Higgs bosons in terms of mixing angles β , α , and $\alpha_{1,2}$,

$$\phi_i^+ = c_{\phi_i}^{H_l^+} H_l^+, \quad h_i = c_{h_i}^{H_l} H_l, \quad \chi_i = c_{\chi_i}^{A_l} A_l, \quad (3.5)$$

where $\{H_l^+\} = (G^+, H^+)$, $\{H_l\} = (\tilde{h}, H, h)$, $\{A_l\} = (G_1, G_2, A)$. The masses of Goldstone bosons are given by $m_{G^+} = M_W$, $m_{G_1} = M_Z$ and $m_{G_2} = M_{Z_H}$ in the Feynman gauge. $c_{\phi_i}^{H_l^+}$, $c_{h_i}^{H_l}$, and $c_{\chi_i}^{A_l}$ satisfy

$$\sum_l c_{\phi_i}^{H_l^+} c_{\phi_j}^{H_l^+} = \delta_{ij}, \quad \sum_l c_{h_i}^{H_l} c_{h_j}^{H_l} = \delta_{ij}, \quad \sum_l c_{\chi_i}^{A_l} c_{\chi_j}^{A_l} = \delta_{ij}, \quad (3.6)$$

$$\sum_i c_{\phi_i}^{H_l^+} c_{\phi_i}^{H_m^+} = \delta_{lm}, \quad \sum_i c_{h_i}^{H_l} c_{h_i}^{H_m} + c_{h_\Phi}^{H_l} c_{h_\Phi}^{H_m} = \delta_{lm}, \quad \sum_i c_{\chi_i}^{A_l} c_{\chi_i}^{A_m} + c_{\chi_\Phi}^{A_l} c_{\chi_\Phi}^{A_m} = \delta_{lm}. \quad (3.7)$$

Each mixing angle is given in Eqs. (2.7), (2.9), and (2.11).

Let us discuss the constraints on the loop corrections to the EWPOs in terms of the S , T , and U parameters defined as [51]

$$\alpha(M_Z^2)T = \alpha(M_Z^2)T_{\text{2HDM}} + \frac{\Delta\Pi_{WW}(0)}{M_W^2} - \frac{\Delta\Pi_{ZZ}(0)}{M_Z^2}, \quad (3.8)$$

$$\frac{\alpha(M_Z^2)}{4s_W^2 c_W^2} S = \frac{\alpha(M_Z^2)}{4s_W^2 c_W^2} S_{\text{2HDM}} + \frac{\Delta\Pi_{ZZ}(M_Z^2) - \Delta\Pi_{ZZ}(0)}{M_Z^2}, \quad (3.9)$$

$$\frac{\alpha(M_Z^2)}{4s_W^2} (S + U) = \frac{\alpha(M_Z^2)}{4s_W^2} (S_{\text{2HDM}} + U_{\text{2HDM}}) + \frac{\Delta\Pi_{WW}(M_W^2) - \Delta\Pi_{WW}(0)}{M_W^2}, \quad (3.10)$$

where $\alpha(M_Z^2)$ is the fine-structure constant at the scale, M_Z , and $(s_W, c_W) = (\sin \theta_W, \cos \theta_W)$ are defined by the Weinberg angle, θ_W . $S_{2\text{HDM}}$, $T_{2\text{HDM}}$ and $U_{2\text{HDM}}$ are the parameters in the ordinary 2HDMs, which could be found in Refs. [59, 60]. The new gauge boson Z_H and the extra scalar boson \tilde{h} in our model make new one-loop contributions to the vacuum polarizations of gauge fields, denoted by $(\Delta\Pi_{WW,ZZ})$. Their explicit expressions up to the $O(\xi)$ corrections are given by

$$\begin{aligned}\Delta\Pi_{WW}(k^2) = & \frac{\alpha}{4\pi s_W^2} \{ (c_{\phi_i}^{H_L^+} c_{h_i}^{H_l} c_{\phi_j}^{H_L^+} c_{h_j}^{H_l}) B_{22}(k^2; m_{H_l}^2, m_{H_L^+}^2) \\ & - \cos^2(\beta - \alpha) B_{22}(k^2; m_H^2, M_W^2) - \sin^2(\beta - \alpha) B_{22}(k^2; m_h^2, M_W^2) \\ & - \sin^2(\beta - \alpha) B_{22}(k^2; m_H^2, m_{H^+}^2) - \cos^2(\beta - \alpha) B_{22}(k^2; m_h^2, m_{H^+}^2) \\ & + \frac{\gamma^2}{1 + \gamma^2} B_{22}(k^2; m_{H^+}^2, M_{Z_H}^2) - \frac{\gamma^2}{1 + \gamma^2} B_{22}(k^2; m_{H^+}^2, m_A^2) \\ & - M_W^2 \left(\frac{v_i v_j}{v^2} c_{h_i}^{H_l} c_{h_j}^{H_l} \right) B_0(k^2; M_W^2, m_{H_l}^2) \\ & + M_W^2 \cos^2(\beta - \alpha) B_0(k^2; M_W^2, m_H^2) + M_W^2 \sin^2(\beta - \alpha) B_0(k^2; M_W^2, m_h^2) \} \\ & - M_W^2 \frac{\alpha_H}{4\pi} \left(\frac{v_i}{v} q_{H_i} c_{\phi_i}^{H_L^+} \right)^2 B_0(k^2; m_{H_l^+}^2, M_{Z_H}^2),\end{aligned}\tag{3.11}$$

$$\begin{aligned}\Delta\Pi_{ZZ}(k^2) = & \frac{\alpha}{4\pi s_W^2 c_W^2} \{ (c_{\chi_i}^{A_m} c_{h_i}^{H_l} c_{\chi_j}^{A_m} c_{h_j}^{H_l}) B_{22}(k^2; m_{A_m}^2, m_{H_l}^2) \\ & - \cos^2(\beta - \alpha) B_{22}(k^2; M_Z^2, m_H^2) - \sin^2(\beta - \alpha) B_{22}(k^2; M_Z^2, m_h^2) \\ & - \sin^2(\beta - \alpha) B_{22}(k^2; m_A^2, m_H^2) - \cos^2(\beta - \alpha) B_{22}(k^2; m_A^2, m_h^2) \\ & - M_Z^2 \left(\frac{v_i v_j}{v^2} c_{h_i}^{H_l} c_{h_j}^{H_l} \right) B_0(k^2; M_Z^2, m_{H_l}^2) \\ & + M_Z^2 \cos^2(\beta - \alpha) B_0(k^2; M_Z^2, m_H^2) + M_Z^2 \sin^2(\beta - \alpha) B_0(k^2; M_Z^2, m_h^2) \} \\ & - M_Z^2 \frac{\alpha_H}{\pi} \left(\frac{v_i}{v} q_{H_i} c_{h_i}^{H_l} \right)^2 B_0(k^2; m_{H_l}^2, M_{Z_H}^2),\end{aligned}\tag{3.12}$$

which are used for phenomenological analyses of the EWPOs. We have defined a new parameter γ for convenience:

$$\gamma = \frac{v}{v_\Phi} \cos \beta \sin \beta.\tag{3.13}$$

The extra corrections additionally depend on the mixing $(\alpha_{1,2})$ among the CP-even scalar bosons, the mass of the extra scalar boson $(m_{\tilde{h}})$, and the Z_H mass and its gauge coupling, (M_{Z_H}, g_H) . The explicit expressions of the functions B_0 and B_{22} can be found in Ref. [59].

3.6 Analysis in 2HDMs with $U(1)_H$ Gauge Symmetry

Here, we discuss the bounds from EWPOs in the 2HDMs with $U(1)_H$ Higgs gauge symmetry. For the numerical analysis, we use the following input parameters: $M_Z = 91.1875$ GeV, $M_W = 80.381$ GeV, $\sin^2 \theta_W = 0.23116$, $\alpha(M_Z) = 1/(127.944)$, and $m_h = 126$ GeV. According to the recent LHC results, the bounds on S , T , and U parameters are given by [61, 62]

$$S = 0.03 \pm 0.10, \quad T = 0.05 \pm 0.12, \quad U = 0.03 \pm 0.10,\tag{3.14}$$

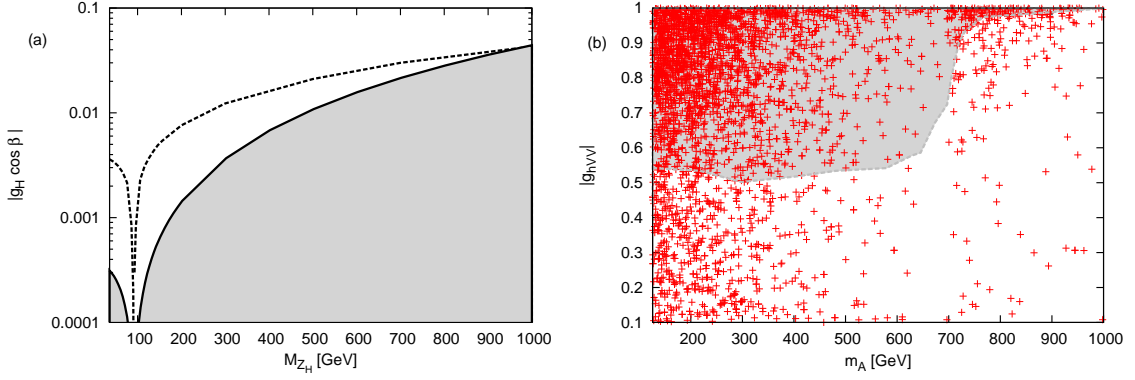


Figure 1. Bounds on M_{Z_H} , $g_H \cos \beta$, g_{hVV} and m_A in the 2HDMs. In the left panel, the gray region satisfies $\sin \xi \leq 10^{-3}$ coming from the collider experiments while the dashed line is the upper limit coming from the ρ parameter and Γ_Z . In the right panel, the gray region is the allowed one for the type-I 2HDM with $g_{hVV} = \sin(\beta - \alpha)$ and $\alpha_1 = \alpha_2 = 0$. The red points are allowed in the 2HDM with $U(1)_H$.

with $m_h^{\text{ref}} = 126$ GeV and $m_t^{\text{ref}} = 173$ GeV. The correlation coefficients are $+0.89_{ST}$, -0.54_{SU} , and -0.83_{TU} .[¶]

In Figs. 1 and 2, the allowed regions within 90% C.L. of S , T , and U parameters are presented in the type-I 2HDM with $q_{H_1} = q_\Phi = 1$ and $q_{H_2} = 0$. The parameters are scanned in the following regions: $1 \leq \tan \beta \leq 100$, $90 \text{ GeV} \leq m_{H^\pm} \leq 1000 \text{ GeV}$, $126 \text{ GeV} \leq m_A, m_H, m_{\tilde{h}} \leq 1000 \text{ GeV}$, and $-1000 \text{ GeV} \leq \mu \leq 1000 \text{ GeV}$. The constraints on the vacuum stability, unitarity and perturbativity introduced in the subsections 3.1 are imposed. The bound from $b \rightarrow s\gamma$ is assigned based on Ref. [44]. Light charged Higgs is constrained by the bound on exotic top decay $t \rightarrow H^\pm b$ [41–43] and the decay widths of $H, \tilde{h} \rightarrow VV$ ($V = W, Z$) are enough small to avoid the bounds in the collider experiments [63].

In Figs. 1 (a) and (b), we show the bounds (a) on M_{Z_H} and $g_H \cos \beta$ and (b) on $g_{hVV} = \sin(\beta - \alpha) \cos \alpha_1$ and m_A in the type-I 2HDM with $U(1)_H$, respectively. Here g_{hVV} is the h - V - V ($V = W, Z$) coupling normalized to the SM coupling. In Fig. 1 (a), the gray region satisfies the collider bound, $\sin \xi \leq 10^{-3}$, mainly from the Drell-Yan process at the LHC and the dashed line corresponds to the upper limit on the constraints coming from the ρ parameter and Γ_Z . In the region $M_{Z_H} \lesssim 1 \text{ TeV}$, the collider bound is stronger than the bound from the ρ parameter and Γ_Z . We note that we include the one-loop corrections involving Z_H to S , T , and U , where $126 \text{ GeV} \leq M_{Z_H} \leq 1000 \text{ GeV}$ and $0 \leq |g_H| \leq 4\pi$. The tree-level contribution to the T parameter is also considered but it just yields the deviation, $|\Delta T| \lesssim 0.01$.

In Fig. 1 (b), the gray region is allowed for g_{hVV} and m_A in the ordinary type-I 2HDM, where $\alpha_1 = \alpha_2 = 0$ and Z_H and Φ are decoupled. If the pseudoscalar mass is heavy, g_{hVV} should be close to one so that the Higgs signal around 126 GeV should be SM-like. The red points are allowed in the 2HDM with $U(1)_H$ with $\sin \xi \leq 10^{-3}$. We note that the small

[¶]Fixing $U = 0$, $S = 0.05 \pm 0.09$ and $T = 0.08 \pm 0.07$ with the correlation coefficient $+0.91$.

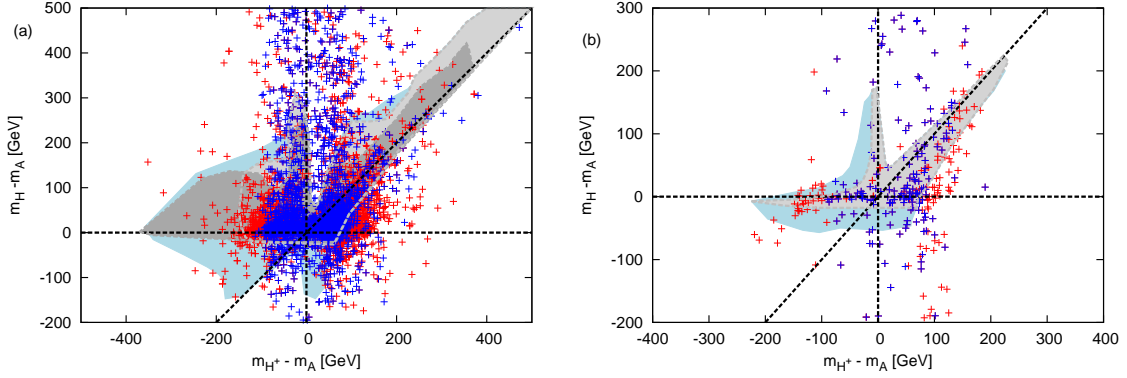


Figure 2. Bounds on $m_{H^+} - m_A$ and $m_H - m_A$ in the 2HDMs. The gray (blue) regions are allowed in the ordinary type-I 2HDM (with $|\lambda_5| \leq 1$). In the left panel, $126 \text{ GeV} \leq m_A < 700 \text{ GeV}$ is chosen and the gray region is divided to the two mass regions: $126 \text{ GeV} \leq m_A < 300 \text{ GeV}$ (gray) and $300 \text{ GeV} \leq m_A < 700 \text{ GeV}$ (dark gray). In the right panel, $700 \text{ GeV} \leq m_A \leq 1000 \text{ GeV}$ is chosen. The red (blue) points are allowed in the type-I 2HDM with $U(1)_H$ without (with) the conditions: $g_{hVV} \geq 0.9$ and $g_{htt} \geq 0.9$. Three dashed lines corresponds to the ones for $m_{H^+} = m_A$, $m_H = m_A$, and $m_{H^+} = m_H$.

g_{hVV} region is also allowed due to an extra factor $\cos \alpha_1$ in g_{hVV} . The small g_{hVV} would reduce the production rate of the SM-like Higgs boson and the partial decay width of h to the EW gauge bosons.

In Fig. 2, we show the bounds on the mass differences among m_A , m_H and m_{H^+} . In Fig. 2 (a), m_A is less than 700 GeV, and the (dark) gray region satisfies $126 \text{ GeV} \leq m_A < 300 \text{ GeV}$ ($300 \text{ GeV} \leq m_A < 700 \text{ GeV}$). In Fig. 2 (b), m_A is within $700 \text{ GeV} \leq m_A \leq 1000 \text{ GeV}$. The gray region is allowed for all the constraints in the ordinary type-I 2HDM with $\alpha_1 = \alpha_2 = 0$ and $\lambda_5 = 0$. As we see in Appendix A, we can realize such small mixings assuming very small $\tilde{\lambda}_1$, $\tilde{\lambda}_2$ and μ or very large v_Φ .

The light blue region corresponds to the ordinary 2HDM with non-zero λ_5 ($|\lambda_5| \leq 1$). In the case of the 2HDMs with $\lambda_5 = 0$, the vacuum stability requires the relation (3.2). On the other hand, non-zero λ_5 modifies the relation and, especially, negative λ_5 pushes the lower bound on m_H down, so that the wider region is allowed in Figs. 1 and 2.

As we see in Fig. 2, each scalar mass could become different. However, it seems that at least two of them should be close to each other in the typical 2HDM with small λ_5 . The heavier pseudoscalar mass requires the smaller mass difference.

In our 2HDM with \tilde{h} and Z_H , the strict bounds could be evaded because of the contributions of the extra particles. The red and blue points are allowed in the type-I 2HDM with $U(1)_H$ and the additional constraints, $g_{hVV} \geq 0.9$ and $g_{htt} \geq 0.9$, are imposed on the blue points. Here g_{htt} is the h - t - \bar{t} coupling normalized to the SM coupling and it is given by $g_{htt} = \cos \alpha_1 \cos \alpha / \sin \beta$ in the type-I 2HDM with $U(1)_H$. Once Φ is added and h_Φ mixes with h_1 and h_2 , the relation (3.2) is discarded, so that the red (blue) points exist outside of the gray region, when h_Φ and Z_H reside in the $O(100)$ GeV scale. In particular, the predictions of the masses of the CP-even scalars are modified, so that $m_H - m_A$ would

have larger allowed region, compared with $m_{H^+} - m_A$. Even if the SM Higgs search limits the normalized h - V - V and h - t - \bar{t} couplings, the mass difference could not be constrained strongly as shown in the region of the blue points.

The constraints from EWPOs could easily be applied to the other type 2HDMs by changing the experimental constraints on the charged Higgs mass. For example, $b \rightarrow s\gamma$ gives the lower bound on $m_{H^+} \gtrsim 360$ GeV in the type-II 2HDMs [44].

4 Collider phenomenology of the Higgs bosons

4.1 Analysis strategies

In this section, we consider collider phenomenology of the Higgs bosons, in particular, focusing on the SM-like Higgs boson. For the calculation of the decay rates of the neutral Higgs bosons, we use the HDECAY [64] with corrections to Higgs couplings to the SM fermions and gauge bosons and with inclusion of the charged Higgs contribution to the $h \rightarrow \gamma\gamma$ and $h \rightarrow Z\gamma$ decays.

There are 10 parameters in the potential neglecting the Z_H boson effects at the EW scale, and one of them is fixed by the SM-like Higgs boson mass $m_h \sim 126$ GeV. We choose the other 9 parameters as $\tan\beta$, m_A , dm_{H^+} , dm_H , $m_{\tilde{h}}$, α , α_1 , α_2 , and v_ϕ , where $dm_{H^+}(dm_H) = m_{H^+}(m_H) - m_A$ is the mass difference between the charged Higgs (heavy Higgs) and pseudoscalar Higgs boson. In this analysis, we choose each parameter region as follows: $1 \leq \tan\beta \leq 100$, $126 \text{ GeV} \leq m_A \leq 1 \text{ TeV}$, $|dm_{H^+,H}| \leq 200 \text{ GeV}$, $0 \leq \alpha, \alpha_{1,2} \leq 2\pi$, $126 \text{ GeV} \leq m_{\tilde{h}} \leq 1 \text{ TeV}$, $0 \text{ GeV} \leq v_\phi \leq 3 \text{ TeV}$, respectively.^{||}

In order to compare our models with the Higgs data at the LHC, we consider the signal strength μ for each decay mode i of the SM-like Higgs boson with the production tag j , which is defined by

$$\mu_j^i = \frac{\sigma(pp \rightarrow h)_{2\text{HDM}}^j \text{Br}(h \rightarrow i)_{2\text{HDM}}}{\sigma(pp \rightarrow h)_{\text{SM}}^j \text{Br}(h \rightarrow i)_{\text{SM}}}, \quad (4.1)$$

where $\sigma(pp \rightarrow h)^j$ means the production cross section for the SM-like Higgs boson with the production tag j and $\text{Br}(h \rightarrow i)$ is the branching ratio of the SM-like Higgs boson decay into the i state. Here $j = gg, Vh$, or VVh , which correspond to the gg fusion production, vector boson associated production, and vector boson fusion production tag, respectively. Finally $i = \gamma\gamma, WW, ZZ$, or $\tau\tau$, depending on the decay channels.

The search for the SM Higgs boson also constrains the mass and couplings of the heavy Higgs boson. In high mass region greater than 200 GeV, the main search mode is $h \rightarrow ZZ \rightarrow 4l$ [65]. For the SM-like Higgs boson, the lower limit for the Higgs boson mass is about 650 GeV and 300 GeV for the gg fusion production and $VVh + Vh$ production, respectively. More detailed analysis is given in Ref. [65]. For a Higgs boson H , the upper bound on the signal strength, $\mu_{VVH,VH}^{ZZ}$ in the $VVH + VH$ production is about one or less for $m_H > 200$ GeV while the bound on μ_{gg}^{ZZ} is about $0.1 \sim 1$ for $200 \text{ GeV} < m_H < 1 \text{ TeV}$.

^{||}The larger mass-scale region could be considered, but they relate to the SM-Higgs signals indirectly through the bounds from the EWPOs and theoretical constraints, as we discuss in Sec. 3. Hence, they would not change our results in this section.

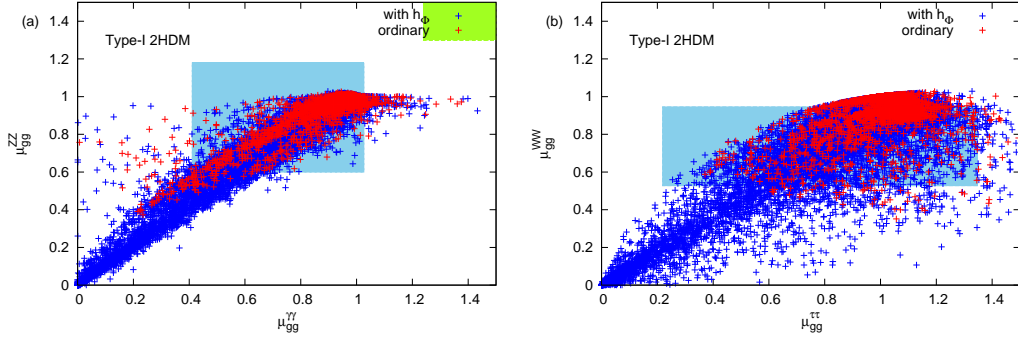


Figure 3. (a) $\mu_{gg}^{\gamma\gamma}$ vs. μ_{gg}^{ZZ} and (b) $\mu_{gg}^{\tau\tau}$ vs. μ_{gg}^{WW} in the ordinary type-I 2HDM (red) and type-I 2HDM with Φ (blue). The effect of Z_H boson is assumed to be small enough to be ignored. The skyblue and green regions are the allowed ones at CMS and ATLAS in the 1σ level.

in the gg fusion production, which varies according to m_H . From the SM Higgs search for $m_H \leq 200$ GeV, we get the constraint on the signal strength $\mu_{gg}^{ZZ} < 0.1 \sim 0.5$ whose bound depends on m_H . We impose these bounds on the heavy Higgs boson H .

In this work, we consider two distinct cases in our Type-I 2HDM with $U(1)_H$ gauge symmetry:

- First, we consider the Type-I 2HDM with $U(1)_H$, assuming that Z_H is decoupled from the low energy Higgs physics. Then, the extra contribution is from only the extra Higgs scalar, and the effect is parametrized by $m_{\tilde{h}}$ and $\alpha_{1,2}$.
- Secondly, we consider the Type-I 2HDM with $U(1)_H$, including Z_H contribution. The charge assignment is fermiophobic by setting $u = d = 0$. In this case the Z_H boson couples with the SM fermions only through the Z - Z_H mixing, and it contributes to the EWPOs.

We compare each case with the ordinary type-I 2HDM by setting $\alpha_{1,2} = 0$ and omitting the singlet scalar Φ and Z_H . We note there is no λ_5 term in the Higgs potential in this case, as we mentioned in the previous section.

4.2 2HDM with the extra singlet scalar

In this section, we consider the type-I 2HDM with the extra singlet scalar field, h_Φ , where we assume that the imaginary part of Φ is eaten by Z_H and the effects of the $U(1)_H$ gauge boson are small enough to be ignored. This could easily be achieved with an assumption of the heavy Z_H mass and small g_H , namely in the limit of large v_Φ .

We show the scattered plots for $\mu_{gg}^{\gamma\gamma}$ and μ_{gg}^{ZZ} in Fig. 3(a), and for $\mu_{gg}^{\tau\tau}$ and μ_{gg}^{WW} in Fig. 3(b), respectively. The red points are allowed in the ordinary type-I 2HDM, whereas the blue points are consistent with the type-I 2HDM with h_Φ , respectively. The skyblue and green regions are consistent with the Higgs signal strengths reported by CMS and ATLAS Collaborations within the 1σ range, respectively, where $\mu_{gg,\text{CMS}}^{\gamma\gamma} = 0.70^{+0.33}_{-0.29}$, $\mu_{gg,\text{ATLAS}}^{\gamma\gamma} = 1.6 \pm 0.4$, $\mu_{gg,\text{CMS}}^{ZZ} = 0.86^{+0.32}_{-0.26}$, and $\mu_{gg,\text{ATLAS}}^{ZZ} = 1.8^{+0.8}_{-0.5}$. Each signal strength at CMS is consistent with that at ATLAS within the 2σ 's.

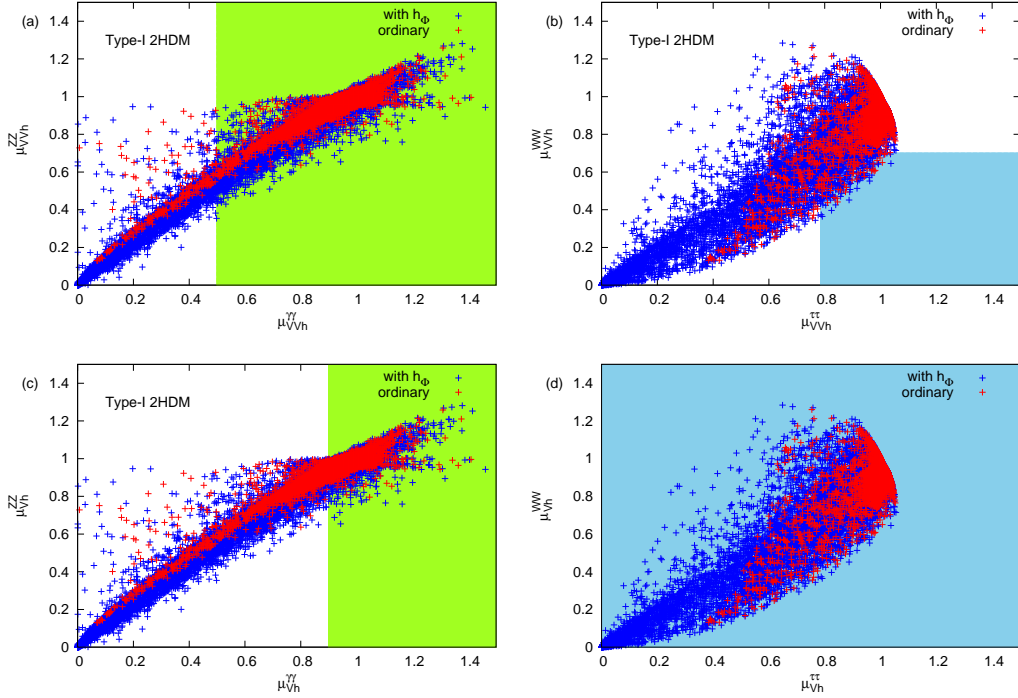


Figure 4. (a) $\mu_{VVh}^{\gamma\gamma}$ vs. μ_{VVh}^{ZZ} , (b) $\mu_{VVh}^{\tau\tau}$ vs. μ_{VVh}^{WW} , (c) $\mu_{Vh}^{\gamma\gamma}$ vs. μ_{Vh}^{ZZ} , and (d) $\mu_{Vh}^{\tau\tau}$ vs. μ_{Vh}^{WW} in the ordinary type-I 2HDM (red) and type-I 2HDM with h_Φ (blue). The effect of Z_H boson is assumed to be small enough to be ignored. The skyblue and green regions are the allowed ones at CMS and ATLAS in the 1σ level.

The SM point is $\mu_{gg}^{\gamma\gamma,ZZ,WW,\tau\tau} = 1$, which is in agreement with the CMS data, but the ATLAS data are consistent only at the 2σ level. In the ordinary 2HDM, the allowed points are in the regions of $\mu_{gg}^{\gamma\gamma} \lesssim 1.4$ and $0.4 \lesssim \mu_{gg}^{ZZ} \lesssim 1.1$. In the 2HDM with h_Φ the allowed region is wider in the $gg \rightarrow h \rightarrow ZZ$ process: $0 \lesssim \mu_{gg}^{ZZ} \lesssim 1.1$. Both 2HDMs contain the SM point $\mu = 1$, and the CMS data for $\mu_{gg}^{\gamma\gamma}$ and μ_{gg}^{ZZ} , but only the edge of the allowed region is barely consistent with the ATLAS data in the 2σ level.

For $\mu_{gg}^{\tau\tau}$ both models predict a large allowed region from 0 (0.4) to 1.5 or larger so that it is difficult to constrain the parameters in the 2HDMs using only $\mu_{gg}^{\tau\tau}$.

In the ordinary 2HDM $0.4 \lesssim \mu_{gg}^{WW} \lesssim 1$ is allowed, whereas much wider region $0 \lesssim \mu_{gg}^{WW} \lesssim 1$ is allowed in the 2HDM with h_Φ . The allowed region in the 2HDM with h_Φ is much broader than that in the ordinary 2HDM.

As shown in Fig 3, the region of $\mu_{gg}^{ZZ} \lesssim 0.4$ and $\mu_{gg}^{WW} \lesssim 0.4$ is not allowed in the ordinary 2HDM. Hence, if it turns out that the two signal strengths were less than 0.4, one might be able to conclude that the 2HDM with h_Φ is more favored than the ordinary 2HDM. However, if it turns out that each signal strength is close to the SM point, the 2HDM with h_Φ cannot be distinguished from the ordinary 2HDM as well as the SM. The mixing with the extra CP-even singlet scalar decreases the two signal strengths, so that we could conclude that their upper bounds are $\mu_{gg}^{\gamma\gamma} \lesssim 1.4$ and $\mu_{gg}^{ZZ} \lesssim 1.0$ in the type-I 2HDM with the extra scalar.

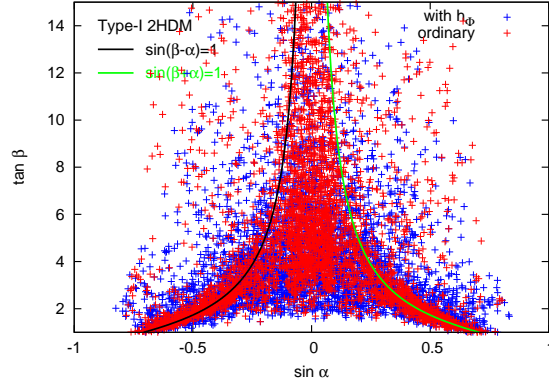


Figure 5. $\sin \alpha$ vs. $\tan \beta$ in the type-I ordinary 2HDM (red) and in the type-I 2HDM with h_Φ (blue). The points are consistent with the CMS data for $\mu_{gg}^{\gamma\gamma}$ and μ_{gg}^{ZZ} in the 1σ level. The black and green lines correspond to the cases $\sin(\beta - \alpha) = 1$ (SM limit) and $\sin(\beta + \alpha) = 1$, respectively.

Fig. 4 shows the scattered plots (a) for $\mu_{VVh}^{\gamma\gamma}$ and μ_{VVh}^{ZZ} , (b) for $\mu_{VVh}^{\tau\tau}$ and μ_{VVh}^{WW} , (c) for $\mu_{Vh}^{\gamma\gamma}$ and μ_{Vh}^{ZZ} , and (d) for $\mu_{Vh}^{\tau\tau}$ and μ_{Vh}^{WW} , respectively. The red points are allowed in the ordinary type-I 2HDM, while the blue ones are in the type-I 2HDM with h_Φ . In the SM, $\mu_{VVh,Vh}^{\gamma\gamma,ZZ,WW,\tau\tau} = 1$ is satisfied. In these figures, the experimental data are consistent with the SM prediction at the 1σ level except μ_{VVh}^{WW} . However, it does not imply any conclusive deviation from the SM since the experimental uncertainties are very large at the moment. As shown in the figures, $\mu_{VVh,Vh}^{ZZ,WW}$ could get much larger than the SM prediction in the parameter regions which increase the branching ratios of $h \rightarrow ZZ$ or $h \rightarrow WW$. We note that the decay widths of the Higgs boson h into ZZ or WW are rescaled by $g_{hVV} = \cos \alpha_1 \sin(\beta - \alpha)$, while those into a fermion pair are by $g_{hff} = \cos \alpha_1 \cos \alpha / \sin \beta$. In the limit of small $\cos \alpha$ or large $\sin \beta$, the branching ratio of the h decay into a $b\bar{b}$ pair could get much smaller than the branching ratio in the SM and as a result, the branching ratios of the h decay into ZZ or WW could be much enhanced.

As shown in Fig 4, the region of $\mu_{VVh,Vh}^{\tau\tau} \lesssim 0.4$ is not allowed in the ordinary 2HDM. Hence, if it turns out that the signal strengths are less than 0.4, one might conclude that the 2HDM with h_Φ is more favored than the ordinary 2HDM. In the region of $\mu_{VVh,Vh} > 0.4$ we cannot distinguish the 2HDM with h_Φ from the ordinary 2HDM. If it turns out that each signal strength is close to the SM point, the 2HDM with h_Φ cannot be distinguished from the ordinary 2HDM as well as the SM.

In Fig. 5, we depict the scattered plot for $\sin \alpha$ and $\tan \beta$. The red and blue points are consistent with the CMS data for $\mu_{gg}^{\gamma\gamma}$ and μ_{gg}^{ZZ} at the 1σ level in the type-I ordinary 2HDM and in the type-I 2HDM with h_Φ , respectively. The black line corresponds to the SM limit $\sin(\beta - \alpha) = 1$ while the green line to $\sin(\beta + \alpha) = 1$. In the ordinary 2HDM and the 2HDM with h_Φ , the allowed points are scattered over the region $|\sin \alpha| \lesssim 0.8$. The region $|\sin \alpha| \gtrsim 0.8$ is forbidden, since the coupling $g_{hff} \sim \cos \alpha / \sin \beta$ to the fermions becomes small for $\tan \beta > 1$. In both models, the allowed regions contain the SM limit $\sin(\beta - \alpha) = 1$ and there is no distinction between the two models. There is no region which agrees with the ATLAS data for $\mu_{gg}^{\gamma\gamma}$ and μ_{gg}^{ZZ} at the 1σ level, but one can obtain a

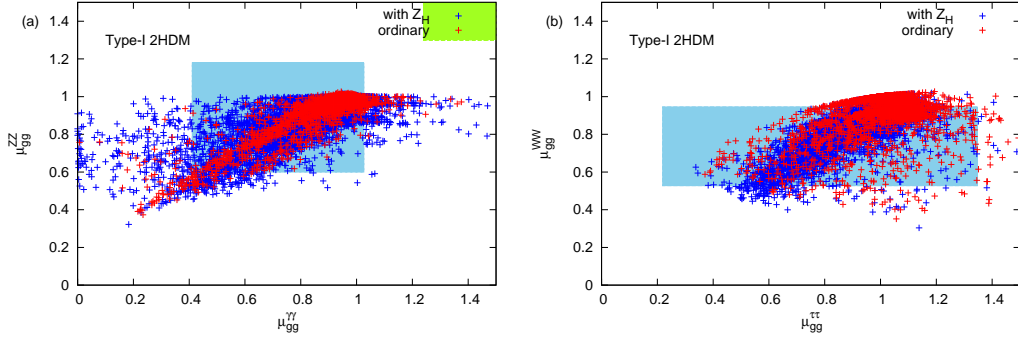


Figure 6. (a) $\mu_{gg}^{\gamma\gamma}$ vs. μ_{gg}^{ZZ} and (b) $\mu_{gg}^{\tau\tau}$ vs. μ_{gg}^{WW} in the ordinary type-I 2HDM (red) and type-I 2HDM with a Z_H (blue). The skyblue and green regions are the allowed ones at CMS and ATLAS in the 1σ level.

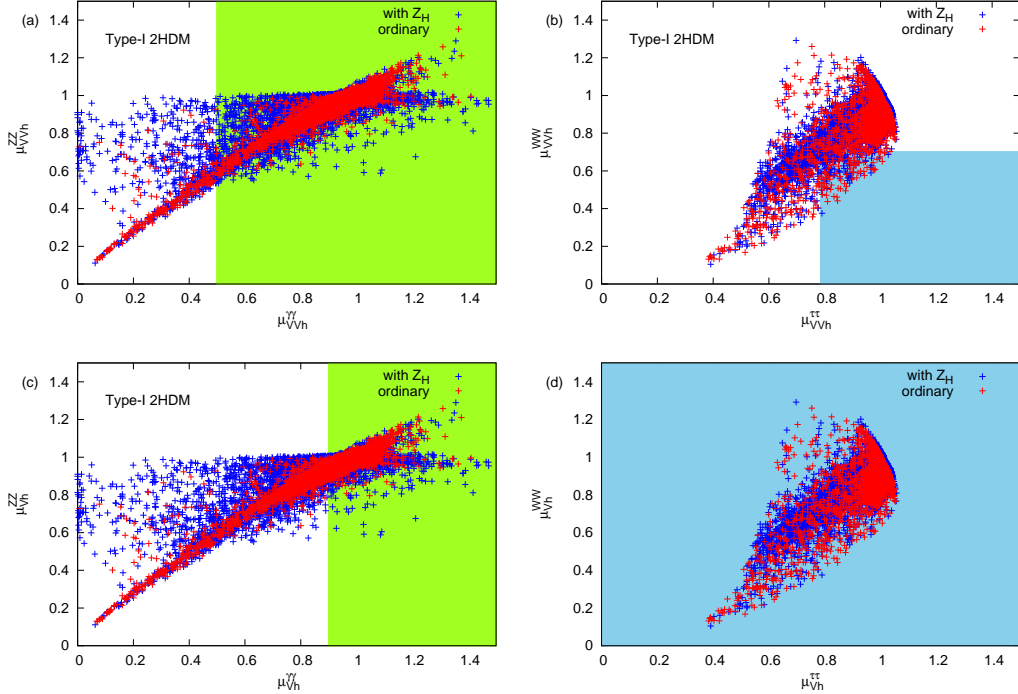


Figure 7. (a) $\mu_{VVh}^{\gamma\gamma}$ vs. μ_{VVh}^{ZZ} , (b) $\mu_{VVh}^{\tau\tau}$ vs. μ_{VVh}^{WW} (c) $\mu_{Vh}^{\gamma\gamma}$ vs. μ_{Vh}^{ZZ} , and (d) $\mu_{Vh}^{\tau\tau}$ vs. μ_{Vh}^{WW} in the ordinary type-I 2HDM (red) and type-I 2HDM with a Z_H (blue). The skyblue and green regions are the allowed ones at CMS and ATLAS in the 1σ level.

similar figure for the ATLAS data at the 2σ level.

4.3 2HDM with the Z_H boson: fermiophobic case

In this section, we discuss the 2HDM with $U(1)_H$ where the $U(1)_H$ gauge boson \hat{Z}_H is fermiophobic, assuming $u = d = 0$ as shown in Table 1. Then the \hat{Z}_H boson does not couple with the SM fermions, but in the mass eigenstate the Z_H boson, which is a mixture of \hat{Z} and \hat{Z}_H , can couple with the SM fermions, and the couplings of the Z boson is modified

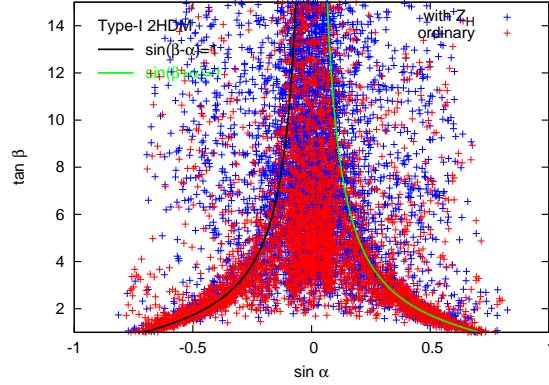


Figure 8. $\sin \alpha$ vs. $\tan \beta$ in the type-I ordinary 2HDM (red) and in the type-I 2HDM with a Z_H boson (blue). The points are consistent with the CMS data for $\mu_{gg}^{\gamma\gamma}$ and μ_{gg}^{ZZ} in the 1σ level. The black and green lines correspond to the cases $\sin(\beta - \alpha) = 1$ (SM limit) and $\sin(\beta + \alpha) = 1$, respectively.

by the mixing angle between \hat{Z} and \hat{Z}_H .

In this model, we have 10 parameters except m_h fixed to 126 GeV. The general model allows the mixing of h_Φ , h_1 and h_2 as shown in Eq. (2.7). However, the analysis of the model is time-consuming and the general feature of mixing between two Higgs doublets and singlet fields would reduce signal strengths as in the previous section. Therefore, we consider no mixing case by setting $\alpha_1 = \alpha_2 = 0$ and compare our results with the typical 2HDM.

We choose the parameter regions as follows: $1 \leq \tan \beta \leq 100$, $126 \text{ GeV} \leq m_A \leq 1 \text{ TeV}$, $|dm_{H^\pm, H}| \leq 200 \text{ GeV}$, $0 \leq \alpha \leq 2\pi$, $126 \text{ GeV} \leq m_{\tilde{h}} \leq 1 \text{ TeV}$. The $U(1)_H$ coupling g_H and the mass of Z_H are chosen to be $0 \leq g_H \leq \sqrt{4\pi}$ and $36 \text{ GeV} \leq M_{Z_H} \leq 1 \text{ TeV}$, where the low bound for M_{Z_H} is taken to suppress the decay mode $h \rightarrow ZZ_H$. Then, v_Φ is given in terms of parameters: $v_\Phi = [M_{Z_H}^2/g_H^2 - v^2/(1 + \tan^2 \beta)]^{1/2}$. In the range of $M_{Z_H} \leq m_h/2$, h can decay into $Z_H Z_H$. However, in our $U(1)_H$ charge assignment $(1, 1, 0)$ on the Higgs fields (Φ, H_1, H_2) , the branching ratio for $h \rightarrow Z_H Z_H$ is suppressed. Actually for the parameters which pass all experimental constraints, we find that $\text{Br}(h \rightarrow Z_H Z_H) < 10^{-5}$ which can be safely ignored in phenomenological analysis.

We depict the scattered plots for $\mu_{gg}^{\gamma\gamma}$ and μ_{gg}^{ZZ} in Fig. 6(a), and for $\mu_{gg}^{\tau\tau}$ and μ_{gg}^{WW} in Fig. 6(b), respectively. The red and blue points correspond to the ordinary Type-I 2HDM and Type-I 2HDM with the Z_H boson, respectively. The skyblue and green regions are CMS and ATLAS bounds at the 1σ level. As shown in Fig. 6, the 2HDM with the Z_H boson seems to have broader regions of the Higgs signal strengths than those in the ordinary 2HDM, but there is no essential difference. In case of the general mixing between the neutral Higgs bosons, we might be able to distinguish the 2HDM with the Z_H boson from the ordinary 2HDM in some parameter spaces, especially in the region $\mu_{gg}^{ZZ, WW} \lesssim 0.4$. However, this region is inconsistent with the current measurements. Both 2HDMs are consistent with the CMS data at the 1σ level. However, it is difficult to increase $\mu_{gg}^{\gamma\gamma}$ and μ_{gg}^{ZZ} to the ATLAS data in the present models. Therefore the 2HDM with the Z_H boson

are not in agreement with the ATLAS data at the 1σ level.

Fig. 7 shows the scattered plots (a) for $\mu_{VVh}^{\gamma\gamma}$ and μ_{VVh}^{ZZ} , (b) for $\mu_{VVh}^{\tau\tau}$ and μ_{VVh}^{WW} (c) for $\mu_{Vh}^{\gamma\gamma}$ and μ_{Vh}^{ZZ} , and (d) for $\mu_{Vh}^{\tau\tau}$ and μ_{Vh}^{WW} , respectively. The red points are allowed in the ordinary type-I 2HDM while the blue ones are in the 2HDM with the Z_H boson. In the 2HDM with the Z_H boson, $\mu_{VVh,Vh}^{ZZ,WW}$ could get much larger than the SM prediction as shown in the figures. If the mixing between the two Higgs doublet and singlet fields are allowed, broader region with smaller signal strengths would be allowed as in the 2HDM with h_Φ discussed in the previous subsection. The SM points $\mu_{VVh,Vh}^{ZZ,WW} = 1$ are consistent with the (ordinary) 2HDMs at the 1σ level except for μ_{VVh}^{WW} . However the deviation in μ_{VVh}^{WW} is not statistically significant yet because of large experimental errors.

In Fig. 8, we depict the scattered plot for $\sin\alpha$ and $\tan\beta$, where the red and blue points are consistent with the CMS data for $\mu_{gg}^{\gamma\gamma}$ and μ_{gg}^{ZZ} in the 1σ level in the type-I ordinary 2HDM and in the type-I 2HDM with the Z_H boson, respectively. The black line corresponds to the SM limit $\sin(\beta - \alpha) = 1$ while the green line to $\sin(\beta + \alpha) = 1$. As in the 2HDM with h_Φ , the region $|\sin\alpha| \gtrsim 0.8$ is not allowed and there is no difference between the ordinary 2HDM and the 2HDM with $U(1)_H$ Higgs gauge symmetry in the type-I case even though the extra Z_H boson contribution is taken into account. However, in the type-II 2HDMs, one could find apparent distinction between the 2HDMs without $U(1)_H$ Higgs gauge symmetry and with the gauge symmetry [35].

5 Conclusion

Discovery of a SM-like Higgs boson at the LHC has opened a new era in particle physics. It is imperative to answer the question if this new boson is the SM Higgs boson or one of Higgs bosons in an extended model with multi-Higgs fields. The 2HDM is one of the simplest models which extend the SM Higgs sector and is well motivated by MSSM, GUT, etc. In Ref. [7], it was suggested to replace the Z_2 symmetry in the ordinary 2HDM with $U(1)_H$ gauge symmetry, which can easily realize the NFC criterion with proper $U(1)_H$ charge assignments to the two Higgs doublets and the SM chiral fermions. The local $U(1)_H$ symmetry may be the origin of softly broken Z_2 symmetry which has been widely discussed so far.

In this paper, we performed detailed phenomenological analysis of the observed 126 GeV Higgs boson within the Type-I 2HDM with the $U(1)_H$ symmetry proposed in Ref. [7]. We added an extra complex scalar that breaks $U(1)_H$ spontaneously, in order to avoid the strong constraint on the mixing between the Z boson and the extra Z_H boson from EWPOs. Our extension of 2HDMs predicts one extra gauge boson and one extra neutral scalar compared with the 2HDMs with Z_2 symmetry, and allows a large pseudoscalar mass according to the spontaneous $U(1)_H$ symmetry breaking.

Taking into account experimental constraints from the SM-Higgs search, EWPO etc., and theoretical constraints from perturbativity, unitarity, and vacuum stability, we studied the signal strengths in two different cases:

- Case I: Type-I 2HDM with the extra scalar h_Φ , assuming the $U(1)_H$ gauge boson is heavy enough to be decoupled at the EW scale. In this case, the Higgs sector includes

an extra scalar which is a remnant from spontaneous $U(1)_H$ symmetry breaking, and the EWPOs will be affected. We found that the signal strengths in the 2HDMs with h_Φ could be much smaller than those in the 2HDM with Z_2 symmetry in some channels. However, if the signal strengths are close to the SM prediction, it would be nontrivial to distinguish the 2HDM with h_Φ from the 2HDM with Z_2 symmetry with Higgs signal strengths alone, especially when all the signal strengths are observed close to the SM values. In case the signal strengths are bigger than the SM prediction, the extra mixing of CP-even scalars does not help to save type-I 2HDM especially in $h \rightarrow VV$.

- Case II: Type-I 2HDM with the Z_H boson where the $U(1)_H$ boson is fermiophobic. This is the simplest solution to the $U(1)_H$ assignments to the SM chiral fermions listed in Table I. Then, Z_H boson can couple with the SM fermions only through the mixing between the \hat{Z} and \hat{Z}_H bosons. In general, the 2HDM with the Z_H boson allows wider region compared with the 2HDM with Z_2 symmetry, but if the mixing between two Higgs doublets and singlet fields are ignored, there is no essential distinction in the allowed regions from the 2HDM with Z_2 symmetry. In particular, if the signal strengths turn out to be close to the SM prediction, the distinction would be nontrivial from the Higgs search alone. Direct search for extra $U(1)_H$ gauge boson and/or extra neutral scalar would be important in such a case.
- In either case, for a given $\mu^{\gamma\gamma}$, the allowed regions for μ^{WW} and μ^{ZZ} are broader than the ordinary 2HDMs. And $\mu^{\tau\tau}$ in Case I could be smaller than those predicted in the ordinary 2HDMs, but is similar in Case II. On the other hand, it would be difficult to distinguish the ordinary Type-I 2HDM from the model with local $U(1)_H$ gauge symmetry based on the observed 126 GeV Higgs signal strengths alone, if the data are close to the SM predictions. It would be essential to discover the extra scalar bosons and the new gauge boson Z_H in order to tell one from the other.

In this work, we considered only the type-I 2HDMs with $U(1)_H$ gauge symmetry, which are the simplest since they are anomaly-free without any extra fermions as long as we choose suitable $U(1)_H$ charges for the SM chiral fermions as in Table I. In this anomaly-free case without extra fermions, it is difficult to enhance the signal strengths $\mu_{gg}^{\gamma\gamma}$ for example. On the other hand, more general 2HDMs with $U(1)_H$ gauge symmetry would generically have gauge-anomaly, like in $U(1)_B$ or $U(1)_L$ models. This gauge anomaly can be cured by adding extra chiral fermions and/or vector-like fermions, which would contribute to the production and the decay of Higgs boson via extra colored and/or electrically charged new particles in the loop and thus could enhance $\mu_{gg}^{\gamma\gamma}$. It is straightforward to extend the present analysis to other type of 2HDMs with $U(1)_H$ gauge symmetry discussed in Ref. [7], in particular, Type-II 2HDM. These models would have richer structures and be more interesting in theoretical and phenomenological aspects, and we plan to report the phenomenological analysis on such models in future publications [35].

Acknowledgments

We thank Korea Institute for Advanced Study for providing computing resources (KIAS Center for Advanced Computation Abacus System) for this work. This work was supported in part by Basic Science Research Program through the National Research Foundation of Korea (NRF) funded by the Ministry of Education Science and Technology 2011-0022996 (CY), by NRF Research Grant 2012R1A2A1A01006053 (PK and CY), and by SRC program of NRF funded by MEST (20120001176) through Korea Neutrino Research Center at Seoul National University (PK). The work of PK was also supported in part by Simons Foundation and National Science Foundation under Grant No. PHYS-1066293 and the hospitality of the Aspen Center for Physics. PK would like to thank CETUP* (Center for Theoretical Underground Physics and Related Areas), supported by the US Department of Energy under Grant No. DE-SC0010137 and by the US National Science Foundation under Grant No. PHY-1342611, for its hospitality and partial support during the 2013 Summer Program. The work of YO is financially supported by the ERC Advanced Grant project FLAVOUR (267104).

A Mass Matrix of CP-even scalars

The mass matrix for 3 CP-even scalars, M_h^2 , is

$$\begin{pmatrix} M'^2 & M_1'^2 & M_2'^2 \\ M_1'^2 & M_{11}^2 & M_{12}^2 \\ M_2'^2 & M_{12}^2 & M_{22}^2 \end{pmatrix} = \begin{pmatrix} 1 & 0 & 0 \\ 0 & \cos \beta & \sin \beta \\ 0 & -\sin \beta & \cos \beta \end{pmatrix} M_h^2 \begin{pmatrix} 1 & 0 & 0 \\ 0 & \cos \beta & -\sin \beta \\ 0 & \sin \beta & \cos \beta \end{pmatrix}, \quad (\text{A.1})$$

$$M'^2 = \left(\frac{m_3'^2}{v_\Phi \sqrt{2}} - \frac{m_3''^2}{2} \right) v^2 \cos \beta \sin \beta + \lambda_\Phi v_\Phi^2, \quad (\text{A.2})$$

$$M_1'^2 = \tilde{\lambda}_1 v_\Phi v \cos^2 \beta + \tilde{\lambda}_2 v_\Phi v \sin^2 \beta - \frac{m_3'^2}{\sqrt{2}} v \sin 2\beta, \quad (\text{A.3})$$

$$M_2'^2 = (-\tilde{\lambda}_1 v_\Phi v + \tilde{\lambda}_2 v_\Phi v) \cos \beta \sin \beta - \frac{m_3'^2}{\sqrt{2}} v \cos 2\beta, \quad (\text{A.4})$$

$$M_{11}^2 = \lambda_1 v^2 \cos^4 \beta + \lambda_2 v^2 \sin^4 \beta + (\lambda_3 + \lambda_4) \frac{v^2}{2} \sin^2 2\beta, \quad (\text{A.5})$$

$$M_{22}^2 = \frac{m_3^2}{\cos \beta \sin \beta} + (\lambda_1 + \lambda_2) v^2 \cos^2 \beta \sin^2 \beta - (\lambda_3 + \lambda_4) \frac{v^2}{2} \sin^2 2\beta, \quad (\text{A.6})$$

$$M_{12}^2 = -(\lambda_1 \cos^2 \beta - \lambda_2 \sin^2 \beta) \frac{v^2}{2} \sin 2\beta + (\lambda_3 + \lambda_4) \frac{v^2}{2} \sin 2\beta \cos 2\beta, \quad (\text{A.7})$$

with $m_3'^2(v_\Phi) \equiv \partial_\Phi m_3^2(v_\Phi)$ and $m_3''^2(v_\Phi) \equiv \partial_\Phi^2 m_3^2(v_\Phi)$.

When $M_1'^2 = M_2'^2 = 0$ is satisfied, the following relations are satisfied:

$$m_H^2 = M_{11}^2 \cos^2(\alpha - \beta) + M_{22}^2 \sin^2(\alpha - \beta) + M_{12}^2 \sin 2(\alpha - \beta), \quad (\text{A.8})$$

$$m_h^2 = M_{11}^2 \sin^2(\alpha - \beta) + M_{22}^2 \cos^2(\alpha - \beta) - M_{12}^2 \sin 2(\alpha - \beta), \quad (\text{A.9})$$

$$\tan 2(\alpha - \beta) = \frac{2M_{12}^2}{M_{11}^2 - M_{22}^2}, \quad (\text{A.10})$$

$$m_h^2 + m_H^2 - m_A^2 = \lambda_1 v^2 \cos^2 \beta + \lambda_2 v^2 \sin^2 \beta. \quad (\text{A.11})$$

When $\alpha_{1,2}$ are small, the angles are approximately

$$\alpha_1 = \frac{-M_1'^2 \sin(\alpha - \beta) + M_2'^2 \cos(\alpha - \beta)}{M'^2 - m_h^2} + O((\alpha_{1,2})^2), \quad (\text{A.12})$$

$$\alpha_2 = \frac{M_1'^2 \cos(\alpha - \beta) + M_2'^2 \sin(\alpha - \beta)}{M'^2 - m_H^2} + O((\alpha_{1,2})^2). \quad (\text{A.13})$$

References

- [1] G. Aad *et al.* [ATLAS Collaboration], Phys. Lett. B **716**, 1 (2012) [arXiv:1207.7214 [hep-ex]].
- [2] S. Chatrchyan *et al.* [CMS Collaboration], Phys. Lett. B **716**, 30 (2012) [arXiv:1207.7235 [hep-ex]].
- [3] S. Chatrchyan *et al.* [CMS Collaboration], Phys. Rev. Lett. **110** (2013) 081803 [arXiv:1212.6639 [hep-ex]].
- [4] ATLAS Collaboration, ATLAS-CONF-2012-169, CERN, Geneva Switzerland (2012).
- [5] G. C. Branco, P. M. Ferreira, L. Lavoura, M. N. Rebelo, M. Sher and J. P. Silva, Phys. Rept. **516**, 1 (2012) [arXiv:1106.0034 [hep-ph]].
- [6] S. L. Glashow and S. Weinberg, Phys. Rev. D **15** (1977) 1958.
- [7] P. Ko, Y. Omura and C. Yu, Phys. Lett. B **717**, 202 (2012) [arXiv:1204.4588 [hep-ph]].
- [8] F. J. Botella, G. C. Branco and M. N. Rebelo, Phys. Lett. B **687**, 194 (2010) [arXiv:0911.1753 [hep-ph]].
- [9] A. Pich and P. Tuzon, Phys. Rev. D **80**, 091702 (2009) [arXiv:0908.1554 [hep-ph]].
- [10] Y. Kahn, M. McCullough and J. Thaler, arXiv:1308.3490 [hep-ph].
- [11] D. London and J. L. Rosner, Phys. Rev. D **34**, 1530 (1986).
- [12] J. L. Rosner, Phys. Lett. B **387** (1996) 113 [hep-ph/9607207].
- [13] P. Ko, Y. Omura and C. Yu, Phys. Rev. D **85**, 115010 (2012) [arXiv:1108.0350 [hep-ph]].
- [14] P. Ko, Y. Omura and C. Yu, JHEP **1201**, 147 (2012) [arXiv:1108.4005 [hep-ph]].
- [15] P. Ko, Y. Omura and C. Yu, Eur. Phys. J. C **73**, 2269 (2013) [arXiv:1205.0407 [hep-ph]].
- [16] P. Ko, Y. Omura and C. Yu, JHEP **1303**, 151 (2013) [arXiv:1212.4607 [hep-ph]].
- [17] A. Arhrib, M. Capdequi Peyranere, W. Hollik and S. Penaranda, hep-ph/0307391.
- [18] A. Arhrib, W. Hollik, S. Penaranda and M. Capdequi Peyranere, Phys. Lett. B **579**, 361 (2004).

- [19] A. Arhrib, R. Benbrik and N. Gaur, Phys. Rev. D **85**, 095021 (2012) [arXiv:1201.2644 [hep-ph]].
- [20] W. Mader, J. -h. Park, G. M. Pruna, D. Stockinger and A. Straessner, JHEP **1209**, 125 (2012) [arXiv:1205.2692 [hep-ph]].
- [21] D. S. M. Alves, P. J. Fox and N. J. Weiner, arXiv:1207.5499 [hep-ph].
- [22] W. Altmannshofer, S. Gori and G. D. Kribs, Phys. Rev. D **86**, 115009 (2012) [arXiv:1210.2465 [hep-ph]].
- [23] Y. Bai, V. Barger, L. L. Everett and G. Shaughnessy, Phys. Rev. D **87**, 115013 (2013) [arXiv:1210.4922 [hep-ph]].
- [24] J. Bijnens, J. Lu and J. Rathsmann, PoS CHARGED **2012**, 023 (2012) [arXiv:1301.7451 [hep-ph]].
- [25] C. -W. Chiang and K. Yagyu, JHEP **1307**, 160 (2013) [arXiv:1303.0168 [hep-ph]].
- [26] M. Krawczyk, D. Sokolowska and B. Swiezewska, J. Phys. Conf. Ser. **447**, 012050 (2013) [arXiv:1303.7102 [hep-ph]].
- [27] A. Barroso, P. M. Ferreira, R. Santos, M. Sher and J. ao P. Silva, arXiv:1304.5225 [hep-ph].
- [28] A. Dery, A. Efrati, G. Hiller, Y. Hochberg and Y. Nir, JHEP **1308**, 006 (2013) [arXiv:1304.6727 [hep-ph]].
- [29] B. Coleppa, F. Kling and S. Su, arXiv:1305.0002 [hep-ph].
- [30] L. Basso, A. Lipniacka, F. Mahmoudi, S. Moretti, P. Osland, G. M. Pruna and M. Purmohammadi, PoS Corfu **2012**, 029 (2013) [arXiv:1305.3219 [hep-ph]].
- [31] P. M. Ferreira, R. Santos, M. Sher and J. ao P. Silva, arXiv:1305.4587 [hep-ph].
- [32] G. Belanger, B. Dumont, U. Ellwanger, J. F. Gunion and S. Kraml, arXiv:1306.2941 [hep-ph].
- [33] D. Lopez-Val, T. Plehn and M. Rauch, arXiv:1308.1979 [hep-ph].
- [34] C. -Y. Chen, arXiv:1308.3487 [hep-ph].
- [35] Work in progress with P. Ko, Y. Omura, and C. Yu.
- [36] H. -S. Lee and M. Sher, Phys. Rev. D **87**, 115009 (2013) [arXiv:1303.6653 [hep-ph]].
- [37] S. Kanemura, T. Kasai and Y. Okada, Phys. Lett. B **471**, 182 (1999) [hep-ph/9903289].
- [38] A. G. Akeroyd, A. Arhrib and E. -M. Naimi, Phys. Lett. B **490**, 119 (2000) [hep-ph/0006035].
- [39] I. F. Ginzburg and I. P. Ivanov, Phys. Rev. D **72**, 115010 (2005) [hep-ph/0508020].
- [40] G. Abbiendi *et al.* [ALEPH and DELPHI and L3 and OPAL and The LEP working group for Higgs boson searches Collaborations], [arXiv:1301.6065 [hep-ex]].
- [41] G. Aad *et al.* [ATLAS Collaboration], JHEP **1206**, 039 (2012) [arXiv:1204.2760 [hep-ex]].
- [42] S. Chatrchyan *et al.* [CMS Collaboration], JHEP **1207**, 143 (2012) [arXiv:1205.5736 [hep-ex]].
- [43] ATLAS Collaboration, ATLAS-CONF-2013-090, “21st International Conference on Supersymmetry and Unification of Fundamental Interactions,” Trieste, Italy, 26 - 31 Aug 2013.
- [44] T. Hermann, M. Misiak and M. Steinhauser, JHEP **1211**, 036 (2012) [arXiv:1208.2788 [hep-ph]].

- [45] J. P. Lees *et al.* [BaBar Collaboration], Phys. Rev. Lett. **109**, 101802 (2012) [arXiv:1205.5442 [hep-ex]].
- [46] M. E. Peskin and T. Takeuchi, Phys. Rev. D **46**, 381 (1992).
- [47] J. Erler, P. Langacker, S. Munir and E. Rojas, JHEP **0908**, 017 (2009) [arXiv:0906.2435 [hep-ph]].
- [48] C. -W. Chiang, Y. -F. Lin and J. Tandean, JHEP **1111**, 083 (2011) [arXiv:1108.3969 [hep-ph]].
- [49] K. S. Babu, C. F. Kolda and J. March-Russell, Phys. Rev. D **54**, 4635 (1996) [hep-ph/9603212].
- [50] K. S. Babu, C. F. Kolda and J. March-Russell, Phys. Rev. D **57**, 6788 (1998) [hep-ph/9710441].
- [51] J. Beringer *et al.* (Particle Data Group), Phys. Rev. D **86**, 010001 (2012).
- [52] M. S. Carena, A. Daleo, B. A. Dobrescu and T. M. P. Tait, Phys. Rev. D **70**, 093009 (2004) [hep-ph/0408098].
- [53] t. S. Electroweak [LEP and ALEPH and DELPHI and L3 and OPAL and LEP Electroweak Working Group and SLD Electroweak Group and SLD Heavy Flavor Group Collaborations], hep-ex/0312023.
- [54] J. Alcaraz *et al.* [ALEPH and DELPHI and L3 and OPAL and LEP Electroweak Working Group Collaborations], hep-ex/0612034.
- [55] ATLAS Collaboration, ATLAS-CONF-2013-017, CERN, Geneva Switzerland (2013).
- [56] CMS Collaboration, CMS-PAS-EXO-12-061, CERN, Geneva Switzerland (2012).
- [57] W. Grimus, L. Lavoura, O. M. Ogreid and P. Osland, J. Phys. G **35**, 075001 (2008) [arXiv:0711.4022 [hep-ph]].
- [58] W. Grimus, L. Lavoura, O. M. Ogreid and P. Osland, Nucl. Phys. B **801**, 81 (2008) [arXiv:0802.4353 [hep-ph]].
- [59] H. -J. He, N. Polonsky and S. -f. Su, Phys. Rev. D **64**, 053004 (2001) [hep-ph/0102144].
- [60] S. Kanemura, Y. Okada, H. Taniguchi and K. Tsumura, Phys. Lett. B **704**, 303 (2011) [arXiv:1108.3297 [hep-ph]].
- [61] M. Baak, M. Goebel, J. Haller, A. Hoecker, D. Kennedy, R. Kogler, K. Moenig and M. Schott *et al.*, Eur. Phys. J. C **72**, 2205 (2012) [arXiv:1209.2716 [hep-ph]].
- [62] M. Baak and R. Kogler, arXiv:1306.0571 [hep-ph].
- [63] S. Chatrchyan *et al.* [CMS Collaboration], [arXiv:1304.0213 [hep-ex]].
- [64] A. Djouadi, J. Kalinowski and M. Spira, Comput. Phys. Commun. **108**, 56 (1998) [hep-ph/9704448].
- [65] ATLAS Collaboration, ATLAS-CONF-2013-013, CERN, Geneva Switzerland (2012).